Charles University in Prague
Faculty of Science
Department of Genetics and Microbiology

Programme: Biology
Branch: Genetics, Molecular Biology and Virology

Bc. Tomáš Galica

Assessing biochemical properties of PDE8A1: Design of experimental system in living cells

Studium biochemických vlastností PDE8A1:
Příprava experimentálního systému v živých buňkách

Master's Thesis

Supervisor: Doc. RNDr. Jan Černý, Ph.D.

Prague 2012

Statement:

I hereby declare that this submission is my own work and that, to the best of my knowledge and belief, it contains no material previously published or written by another person nor material which to a substantial extent has been accepted for the award of any other degree or diploma of the university or other institute of higher learning.

August 29th 2012

Prague

Tomáš Galica

Acknowledgements

I would like to thank my supervisor Jan Černý for providing great space and freedom during work on my Master's Thesis and immesurable help with writing the manuscript. I am deeply grateful to my colleagues from laboratory of cellular immunology and Marek Romášek for the assistence on the hectic final assembly of the thesis. Further more I would like to thank Ondra Šebesta for the patience he had with me while I was trying to master the microscope. I would like to thank Ondra and Eliška for providing shelter during Summer 2012.

Last but definitively not least I would like to thank my family and *B*. for all the support they provided me with.

Abstract

Phosphodiesterases (PDEs), enzymes that hydrolyze cyclic nucleotides, are important components of signal transduction pathways in eukaryotic cells. Second messenger 3'-5'-cyclic adenosine monophosphate (cAMP) is hydrolyzed by specific PDEs. By controlling concentration levels of cAMP in cell, PDEs preserve favorable environment for successful transmission of the cAMP signal. Moreover, PDEs are activated by protein kinase A (PKA) in response to elevated cAMP concentration, which is a feature crucial for signal termination.

PDE8A1 is a high-affinity cAMP-specific IBMX insensitive phosphodiesterase, an enzyme important for cAMP signaling. However, mostly due to a lack of specific inhibitor, its role has not been assessed in detail. This thesis reports cloning of PDE8A1, identification of its posttranslational modifications and subcellular localization, as well as an alternative approach to address PDE biology by the use of cyclase toxin from *Bordetella pertussis*.

Keywords:

phosphodiesterase, cAMP, posttranslational modification, myristoylation, palmitoylation, adenylate cyclase toxin

Abstrakt

Fosfodiesterázy sú dôležitou súčasťou signálnych dráh eukaryotických buniek. Druhý posol 3'-5'-cyklický adenozín monofosfát (cAMP) je hydrolyzovaný špecifickými fosfodiesterázami. Kontrolou hladiny cAMP v bunke fosfodiesterázy zabezpečujú vhodné prostredie pre prenos cAMP signálu. Navyše, ako odpoveď na zvýšenú hladinu cAMP, sú fosfodiesterázy aktivované proteín kinázou A (PKA), čo je vlastnosť dôležitá obzvlášť pre patričné ukončenie signálu.

Fosfodiesteráza 8A (PDE8A1) je vysoko-afinitná cAMP-špecifcká fosfodiesteráza necitlivá k inhibícii pomocou IBMX. Je významný enzýmom pre cAMP signalizáciu, avšak najmä kvôli nedostupnosti PDE8A špecifického inhibítoru, jej úloha ešte nebola detailne preskúmaná ani docenená. Prezentovaná práca zahŕňa klonovanie PDE8A1, identifikáciu jej posttranslačných modifikácii, lokalizáciu na bunkovej úrovni ako aj alternatívny prístup ku skúmania fosfodiesteráz pomocou cyklázového toxínu z *Bordetelly pertussis*.

Kľúčové slová:

fosfodiesteráza, cAMP, posttranslačné modifikácie, myristoylácia, palmitoylácia, adenylátcyklázový toxín

Abbreviations

(m)AKAP	(muscle-specific) A-kinase anchoring protein
AC	Adenylate cyclase
Arnt	aryl hydrocarbon receptor nuclear translocator protein
ATCC	American Type Culture Collection
cAMP	Cyclic adenosine monophosphate
CD	cluster of differentiation
cGMP	Cyclic guanosine monophosphate
CHO cells	Chinese hamster ovary cells
CIAP	Calf-intestinal alkaline phosphatase
cNMP	Cyclic nucleoside monophosphate
CXCL12	chemokine (C-X-C motif) ligand 12
Cya A	adenylate cyclase toxin from Bordetella pertussis
DAPI	4',6-diamidino-2-phenylindole
DMSO	Dimethyl sulfoxide
EDTA	Ethylenediaminetetraacetic acid
EGFP	enhanced green fluorescent protein
EPAC	exchange proteins activated directly by cyclic AMP
ERK kinase	extracellular-signal-regulated kinase
EtBr	Ethidium bromide
FACS	Fluorescence-activated cell sorting
FBS	fetal bovine serum
FRET	Förster (Fluorescence) resonance energy transfer
FSC	Forward Scatter
FSK	forskolin
GAF	c**G**MP-specific phosphodiesterases, **a**denylyl cyclases and **F**hlA
GPCR	G protein coupled receptors
HS DNA polymerase	hot start DNA polymerase
IBMX	3-isobutyl-1-methylxanthine

IPTG	Isopropyl β-D-1-thiogalactopyranoside
LA DNA polymerase	long and accurate DNA polymerase
MEK5	MAP/ERK kinase 5
MEKK	MAP kinase kinase kinase
nt	nucleotide
Oct	octamer transcription factor
ORF	open reading frame
PAK	p21 activated kinases
PAS domain	**P**er, **A**rnt, **S**im domain
PBS	Phosphate buffered saline
PCR	polymerase chain reaction
PDE	Phosphodiesterase
PGE_1	Prostaglandin E1
RACK-1	receptor of activated kinase 1
REC domain	CheY-like phosphoacceptor (or receiver) domain
SOC	Super Optimal broth with Catabolite repression
TAPAS-1 domain	tryptophan anchoring phosphatidicacid selective-binding domain 1
TBE	Tris/ Borate/ EDTA
TNFα	Tumor necrosis factor alpha
TPB	Tryptose Phosphate Broth
TUC	Tris/ Urea/ Calcium

Contents

1 Introduction

Compartmentalization of biological pathways and molecules in eukaryotic cells is a fascinating and widespread phenomenon. Both molecules and signals are likely confined to different compartments, thus allowing biological processes not to constrain or interfere with each other. However, despite enormous extend of the research, some aspects remain controversial or still not assessed.

The thesis presented here extends the research previously conducted in our laboratory (Laboratory of cellular immunology) that identified PDE8A as membrane protein with potential localization to lipid rafts (Falteisek 2008). Previous studies performed by Lukáš Falteisek were focused only on N-terminal segments of the PDE8A protein and determination of their cellular localization. It was decided that characterization of PDE8A1 should include the study of the whole protein and its subcellular localization with regards to compartments of cAMP (production and utilization) and membrane micro-domains (rafts). This decision shaped the main goals of this thesis. First objective was to prepare full-length fluorescently tagged PDE8A1. Second objective was to construct PDE8A1 variants that would carry mutations in signal sequence for N-myristoylation and palmitoylation and verify their cellular localization as was done for the N-terminal segments (Falteisek 2008).

An interesting challenge was to design an experimental system, possibly in living cells, where the role of subcellular localization of PDE8A1 could be assessed. This goal included construction of catalytically inactive PDE8A1 that later would be part of control measurements within the suggested experimental system.

PDE8A1 represents an interesting protein, quite divergent from other members of PDE family, putatively essential for function of various tissues. However, in contrast to related PDE4 is only poorly studied. Aspiration of this thesis is to add a small piece of knowledge to fill this gap. More general, this thesis gives the preliminary data to the long-term fierce discussion about functional relevance of membrane microdomains establishing model system for testing interplay between two raft-localized proteins with opposite functions (cAMP production vs. utilization).

2 Review of available literature

2.1 Phosphodiesterases (PDEs)

Signaling by cyclic nucleotides is a complex process that requires fine tuning with regards to the specific physiological state of any particular cell (Conti and Beavo 2007, Serezani et al 2008). Since PDEs play important role in this widespread mechanism of cellular signalization, it is not surprising that they are subject to this tuning and that this is reflected by the abundance and structural variability of PDE genes and vice versa (Conti and Beavo 2007).

2.1.1 Diversity of PDEs

Already in the seventies there were first observations that phosphodiesterases are diverse in structure and enzymatic properties (Donnelly 1977). Later, during studies focused on the development of immunoprecipitation of calmodulin-phosphodiesterase complexes, different molecular sizes of the isoforms originating in heart or brain tissue were observed (Hansen and Beavo 1982). This observation subsequently led to discovery of another isoform of calmodulin dependent phosphodiesterase in brain tissue (Hansen and Beavo 1986) and formed the basic knowledge about group of PDEs that would later become the PDE1 gene family.

Within years of research, many more genes and proteins were discovered resulting in 11 gene families of mammalian PDEs and approximately a hundred of resulting proteins recognized today (Beavo 2007).

2.1.2 Variability of PDEs in mammals

In human genome, 21 PDE genes have been identified and divided into gene families according to their enzymatic properties and sequence similarity. . Gene families PDEs 1, 2, 3, 10 and 11 lack substrate specificity and hydrolyze both cAMP as well as cGMP with varying efficiency. cGMP is specifically hydrolyzed by PDEs belonging to gene families PDEs 5, 6 and 9, while PDEs 4, 7 and 8 hydrolyze cAMP (Conti and Beavo 2007). PDE8 gene family consists of PDEs that bind specifically cAMP, with high affinity, and are distinguished by their insensitivity to IBMX, a cAMP analogue that successfully inhibits other cAMP specific PDEs (Fisher et al 1998, Soderling et al 1998).

As mentioned above, the fine tuning of cyclic nucleoside signaling mechanisms requires large collection of PDEs with slightly modified localization, protein interactions and enzyme kinetics. In order to meet this requirements, genes coding PDEs are organized in modular fashion enabling numerous exons to be alternatively spliced and give rise to variety of PDEs (Conti and Beavo 2007). PDE4A gene is a good example of this phenomenon, since it contains multiple exons (approximately 15) separated by long stretches of non-coding DNA, that are joined in multiple variants of mRNA and resulting in 7 proteins (Rena et al 2001, MacKenzie et al 2008, Uniprot database). PDE4D gene is also transcribed in at least 9 different mRNAs, to six of which corresponding protein was found in mammalian tissues (Richter et al 2005). For PDE9A there were 20 transcripts reported and similar pattern was observed in other PDE genes, although the numbers are not final, since more are to be discovered and some might prove to be protein non-coding transcripts (Conti and Beavo 2007).

In order to differentiate expression of PDE isoforms mammalian PDE genes contain multiple promoters, what is well documented in the case of PDE4D where there are two verified promoters, one regulating the expression of isoforms PDE4D1/2 and another promoter for PDE4D5, yet still another two predicted promoters need to be confirmed (Le Jeune et al 2002, Vicini and Conti 1997). The extent of expression as well as tissue specific distribution is determined by isoform-specific promoter, in this way is for example achieved limited tissue distribution of PDE4A8 in brain, skeletal muscle and to lesser extent in testis, while another variant, PDE4A10, is present in variety of tissues such as hearth or small intestine (MacKenzie et al 2008, Rena et al 2001). Promoters of PDE genes are localized in introns just upstream of the first exon of the corresponding PDE variant and often lack TATA-box but contain stretches of high GC content and cAMP responsive elements. Their presence allows gene regulation of PDEs on transcription level in response to concentration of cellular cAMP (Le Jeune et al 2002, Vicini and Conti 1997). Presence of multiple promoters in PDE genes specific for particular isoforms corresponds well with their different tissue specific expression, however present knowledge does not cover the intriguing topic of PDE promoters, which are still largely unknown (Houslay et al 2007).

2.1.3 Variable regions of PDEs

In contrast to structure of catalytic domain, which is well conserved among PDEs, both N- and C- terminal regions are highly variable. Variability of N-terminal region is mostly responsible for an amazing diversity of PDE isoforms present within the organism as illustrated by Richter et al 2005 or reviewed by Conti and Beavo 2007. Such extensive diversity is out of scope of this thesis and will be assessed briefly, focusing rather on what is relevant to the main subject of this study (PDE8A and signaling through cAMP), thus PDEs with dual specificity or specificity to cGMP are on the periphery of interest.

Although a phosphorylation site of ERK2 kinase was detected in PDE4D in the C-terminal portion of the catalytic domain (MacKenzie et al 2000), only very limited information is available about the region of PDEs located behind catalytic domain (Conti and Beavo 2007). In contrast numerous regulatory and phosphorylation domains were localized to N-terminal portion of PDEs (Conti and Beavo 2007).

Plethora of functional elements is present in the N-terminal region of PDEs. Dimerization is common among PDEs and although the functional role of oligomerization state of PDEs is not fully understood, regions responsible for dimerization has been mapped to N-terminal segment (Conti and Beavo 2007). However not all PDE genes are known to include oligomerization domains and some isoforms are known to lack this feature at all (Conti and Beavo 2007). In addition to dimerization domains variable regions of PDEs also contain regulatory elements such as ligand binding domains and phosphorylation sites. For example five of the 11 PDE families, PDE2, PDE5, PDE6, PDE10 and PDE11, contain so called GAF domain that are able to allosterically regulate enzymatic activity or facilitate formation upon binding of cNMP (Conti and Beavo 2007). All PDE4 genes codes for conserved protein motif that represents phosphorylation site for PKA, however this motif is not included in all isoforms due to alternative splicing (MacKenzie et al 2002).

Variability of N-terminal region of PDEs is thought to be connected to compartmentalization of cAMP signaling, where particular variant of N-terminus can facilitate the direct association of the concerned PDE with specific signaling circuit (Houslay et al 2007).

This targeting can be achieved by association with different cellular membranes, as it is in the case of PDE4A1, where TAPAS-1 domain facilitates phospholipid binding (Bailie et al 2002). Fine tuning is further achieved by specific binding of TAPAS-1 domain to phosphatidic acid in calcium dependent manner, that could provide link to Ca^{2+} signaling, however once this association is established it is not easily abolished even after chelatation of Ca^{2+} ions. This molecular mechanism can serve as a sort of long term signaling "memory" of particular Ca^{2+} release event (Bailie et al 2002).

Another way of implementing PDEs into specific circuits might be through association with scaffolding proteins such as A-kinase anchor protein (AKAP) or RACK-1 (Houslay et al 2007). PDE4D3 is associated with muscle specific AKAP, but PDE4D5 is not, since the interaction is mediated by the N-terminal segment of PDE4D protein that actually distinguish PDE4D3 from PDE4D5 (Dodge et al 2001). Scaffold protein mAKAP thus brings to proximity PKA activated by elevated levels of cAMP and PDE4D3 capable of hydrolyzing cAMP. Moreover rate of cAMP hydrolysis by PDE4D3 can be altered if specific sites are phosphorylated, eventually by PKA, suggesting a possible negative feedback loop (Dodge et al 2001). Later, after more detailed examination, it was shown that mAKAP indeed forms a signaling module with incorporated negative feedback loop, where presence of PDE4D3 controls the duration of the signal, in the form of PKA activity (Dodge-Kafka et al 2005). While PDE4D3 is associated with mAKAP, the PDE4D5 isoform binds to proteins RACK1 and β-arrestin, and again this interaction mediated by N-terminal segment which allows distinction between isoforms of PDE4D (Lynch et al 2005). Moreover detailed mapping of this interaction domain revealed that binding sites for RACK1 and β-arrestin overlaps in PDE4D5, so that the binding is mutually exclusive (Bolger et al 2006). Thus RACK1 and β-arrestin compete for binding to PDE4D5 and subsequently sequester it in distinct signaling circuits (Bolger et al 2006).

2.1.4 The catalytic domain

Based on the sequence and structure of catalytic domain, 3 classes of PDEs are distinguished (Conti and Beavo 2007, Richter 2002). Class III PDEs are related to purple acid phosphatases and thus considered to belong to a large family of dimetallophosphoesterases. They are to confined to the prokaryotes and their catalytic activity depends on presence of Fe2+ ions in the catalytic site (Richter 2002). PDEs with

class II catalytic domain are known from fungi, slime mold *Dictyostelium discoideum* and bacteria (Conti and Beavo 2007). Detailed study of PDEs of D. discoideum suggests that they form two subgroups, one of which bears a resemblance to metallo-β-lactamases (Bader et al 2007). Most studied are class I PDEs that are present in fungi, protozoans and in metazoans they are the sole class of PDEs (Conti and Beavo 2007). Dealing with classification and distribution of PDEs in different organisms, it should be mentioned that there is not much known about PDEs in plants and although several genes possibly coding for PDEs has been identified, evidence is still lacking (Martinez-Atienza 2007). Known inhibitor of wide spectrum of animal PDEs, IBMX, hastens plant response to potential pathogen, suggesting important functional role of PDEs in plant physiology, however which genes and proteins are responsible for cAMP metabolism in plants remain unclear (Ma et al 2009).

Mammalian PDEs are considered to be very good targets for pharmacological interventions and since rational drug design require knowledge of the structure, for many PDEs resolved 3D-proteins structure is available by now (Conti and Beavo 2007, Wang et al 2008). The catalytic domain of PDEs consists of 17 α-helices that arranged in 3 subdomains that altogether form deep pocket in which the cNMP is bound and subsequently hydrolyzed (Ke 2004). Four areas are distinguished in the deep hydrophobic pocket: a metal-binding site (M site), core pocket (Q pocket), hydrophobic pocket (H pocket) and lid region (L region, Jeon et al 2005). The sequence alignment of PDEs revealed two conserved Hx3Hx24–26E sequences, corresponding with known zinc-binding motifs. Moreover, PDEs has been shown to require divalent cations for catalytic activity, especially presence of zinc at low concentrations is reported to be of high importance (Francis et al 1994). Determination of crystal structure of PDEs revealed that the metal-binding site forms the bottom of the pocket, and bind two metal ions, one of which has been determined to be Zn^{2+} and the other is thought to be Mg^{2+} or Mn^{2+} (Ke 2004, Jeon et al 2005).

An important feature of PDEs is their substrate selectivity for cAMP or cGMP, which is determined by conformation of a glutamine residue within the core pocket area, thus called the glutamine switch (Zhang et al 2004). This particular glutamine can adopt 2 different conformations depending on its surrounding protein structure. Each

conformation prefers either cAMP or cGMP. In nucleotide specific PDEs conformation is imposed to the concerned glutamine residue, thus allowing only binding of only one specific cNMP, while in non-specific PDEs this glutamine is allowed to rotate freely and possibly bind both of the possible cNMP almost without preference (Zhang et al 2004, Fi).

Above mentioned variability of PDEs is also demonstrated by their different vulnerability to variety of small organic molecules, inhibitors of PDEs that are bound to the hydrophobic pocket. Although both PDEs and their inhibitors vary in structure, their interactions share common features (Joen et al 2005). The central ring of the ligand/inhibitor is held on the positions of purine ring of cNMP by so called hydrophobic clamp and interacts with conserved glutamine of the glutamine switch, however inhibitor substances seem to avoid interaction with metal ions on the bottom of the hydrophobic pocket (Joen et al 2005). Inhibitor selectivity is determined by the shape of the hydrophobic pocket, yet whether it is the overall shape or rather specific residues, is a question not fully answered (Ke 2004). However most likely it will be the combination of both, while the contribution of both aspects might differ from case to case. In the case of PDE8a, single mutations of amino acids participating on forming the hydrophobic pocket have been reported to alter the inhibitor selectivity, since mutation of Tyr748 to Phe748 cause otherwise IBMX insensitive PDE8A to be inhibited by it (Wang et al 2008).

Although knowledge about structure of catalytic domain of PDEs still can be expanded, it is by now explored in good detail. In contrast, the structures of both N-terminal and C-terminal regions remain elusive, mostly due to their complicated crystallization and variability (Conti and Beavo 2007).

2.1.5 Evolution of PDEs

Diversity and abundance of PDEs in vertebrates observed today has probably emerged by several rounds of gene, or eventually genome, duplication (Koyanagi et al 1998). Since all animal PDEs known so far contain phosphodiesterase class I catalytic domain shared with yeast PDE2, they are thought to diverge from one ancestral gene with a single domain (Conti and Beavo 2007, prosite). Considering the fact, that in yeasts there is only one PDE of class I and already in freshwater sponge *Ephydatia fluvialis* 4 PDE genes are detected, first duplication of PDE ancestral gene must have occurred early in the evolution between the animal-fungus split and the divergence of porifera and eumetazoa

(Koyanagi et al 1998). Expansion of PDE genes then continues, as is exemplified on the case of PDE4 which is duplicated again after divergence of *Mixiniformes* and before the divergence of teleosts, since further the evolutionary history of PDE genes in other vertebrates differ from that in teleosts (Johnson et al 2010). Early after the first duplications of PDE genes, rapid accumulation of amino acid substitutions was observed, however later when the duplicated genes become more established the mutation pace slowed down (Koyanagi et al 1998). Rapid accumulation of amino acid substitutions is not only sign of distant evolutionary history, since despite human PDE4A8 is highly similar to rat PDE4A8 in nucleotide sequence on protein level there are drastic changes in the length and composition of its N-terminal region, indicating that it must have happened recently after divergence of rodents and primates (b 2005). Moreover this N-terminal region of human PDE4A8 is more similar in sequence to the PDE4B1 of *Sus scrofa* and *Callithrix jacchus* than to PDE4A8 in those species, suggesting recent evolutionary rearrangements (Johnson et al 2010).

In mammals the required diversity of PDE proteome is achieved mostly via alternative splicing (Richter et al 2005), however this is not true in teleosts, where instead of alternative splicing additional duplication of PDE4 genes ensures the required diversity of PDE4 isoforms (Johnson et al 2010). The growing need for finely tuned and complex signaling during the course of animal evolution corresponds with increasing amount of different PDE proteins, achieved both by gene duplication and alternative splicing (Johnson et al 2010, Koyanagi et al 1998, Conti and Beavo 2007, MacKenzie et al 2008).

2.2 Signaling via cAMP

In 1957 Rall, Sutherland and Berthet observed stimulation of liver phosphorylase by a heat stable factor that, as was shown later, contained adenosine, ribose and phosphate in 1:1:1 molar ratio. Moreover this factor was present in fraction of cell lysates that contained membranes after response to addition of hormones. Then when purified factor was added to membrane free fractions of cell lysates it has activated phosphorylase, a physiological response that hormones alone could not elicit. It was the moment, when concept of second messengers was first formed (as reviewed in Beavo and Brunton 2002). Determination of the structure of this heat stable factor has revealed the original second messenger to be 3',5'-cyclic adenosine monophosphate (cAMP; Beavo and Brunton 2002).

Sutherland was awarded a Nobel-prize for his discovery and research of cAMP dependent mechanisms.

The first notion that cAMP signaling might be compartmentalized in the cell comes from studies of Brunton and coworkers (Edwards et al 2011). The cAMP concentration has risen to the same extent in cardiac muscle cell in response to stimulation of either isoprenaline or PGE_1. However only stimulation by isoprenaline activated the glycogen phosphorylase and increased the ventricular pressure. Thus observed physiological response depended rather on the way the cAMP concentration rise was triggered (Hayes et al 1980)

Nowadays the concept of compartmentalized cAMP signaling is an accepted part of a paradigm (Edwards et al 2011). In the following chapter it is reviewed how local gradients of cAMP can be achieved or how is it possible that the cell can accommodate multiple signaling circuits that use the same second messenger.

2.2.1 Architecture of cAMP signaling pathway

Cellular signaling events that implement cAMP can be divided into several steps. First, the signal is triggered and initiates the activation of adenylyl cyclase (AC). Second, generated cAMP transduces the signal to efector protein that results in physiological response. Finaly, the signal is terminated by hydrolyzing cAMP into AMP by PDEs (Serezani et al 2008; Kamenetsky et al 2006).

Conventionally, the first trigger is the binding of extracellular (first) messenger to heptahelical G-protein coupled receptor (GPCR; Serezani et al 2008). There are more than 800 genes coding for GPCRs in human genome that transmits their signal further through heterotrimeric guanine nucleotide binding proteins, also called simply G proteins. Binding of extracellular messenger to GPCRs results in conformational change, that triggers exchange of GDP for GTP in the G-protein thus initiating activation and dissociation of the G_α subunit from the complex (Cotton and Claing 2009). The dissociated Gα subunit interacts with transmembrane adenylyl cyclase that converts ATP into cAMP. There are four major families of G proteins: G_s, $G_{i/o}$, $G_{q/11}$ and $G_{12/13}$ (Cotton and Claing 2009), yet only G_s and $G_{i/o}$ are known to interact with transmembrane adenylyl

cyclase and while G_s promotes generation of cAMP, $G_{i/o}$ suppresses it (Kamenetsky et al 2006).

Adenylyl cyclase (AC) translates the information coming from the cell exterior through G-protein into cAMP signal (Kamanetsky et al 2006). The whole family of ACs consists of 10 genes in the human genome. In addition, alternative splicing has been reported in at least some of their transcripts, thus increasing the diversity of AC proteome. Nine of ten AC genes code for proteins that include transmembrane domain and interact with GPCR. In contrast the last AC gene codes for soluble protein with AC activity that is thought to be regulated by calcium ions and bicarbonate (Kamanetsky et al 2006).

After conversion from ATP by AC, cAMP reaches the effector protein and induces functional changes, resulting in altered activity and subsequently to the physiological response. Three species of proteins are considered to be the effector proteins of cAMP. Protein kinase A (PKA) binds cAMP molecule and then releases its catalytic unit that phosphorylates numerous protein substrates (Kamanetsky et al 2006). Exchange protein directly activated by cAMP (EPAC) promotes the release of GDP and binding to GTP, thus activating small GTPases (Rooij et al 1998) and cyclic nucleotide-gated ion channels translate the cAMP signal into voltage response (Cukkemane et al 2011). Downstream from the effector protein the signaling cascade is branched extensively and includes plenty of processes such as phagocytosis (Ballinger et al 2010), T-cell adhesion (Vang et al 2010), regulation of contraction strength in hearth (Beca et al 2011) or glycogen metabolism (Hayes et al 1980).

Duration of the signal is vital for the proper course of the response thus appropriate termination of the cAMP signal is achieved via hydrolysis of 3’-5’ phosphodiester bond by PDEs (Serazani et al 2008). Since, as stated above, variable processes are controlled by the cAMP signaling cascade. Considering their different nature, different duration and speed of the signal termination is required by each of them and such diversity of requirements is covered by the vast array of PDE isoforms (Conti and Beavo 2007).

The general structure of cAMP signaling pathways is modular in nature, since for any position within the cAMP signaling pathway there is a pool of different proteins and isoforms that could possibly occupy it. Broad pool of available elements allows their

combination into finely tuned signaling circuits that are implemented in variable processes within the cell.

2.2.2 Compartmentalized signaling

The idea of compartmentalized signaling through cAMP after the notion that elevated concentration of cAMP might result in distinct physiological outcomes depending on the agents used to provoke it (Hayes et al 1980, Edwards et al 2011). Then years of research brought significant amounts of biochemical evidence that it is physiologically relevant (Houslay and Adams 2003) and more recently it has become possible to visualize cAMP gradients in living cells (Edwards et al 2011). Advances in fluorescent microscopy techniques and design of genetically encoded florescent probes, especially those implementing principles of Förster resonance energy transfer (FRET) rendered such a visualization possible and broadly available (Edwards et al 2011).

2.2.2.1 Shaping the gradient

Establishing concentration gradient of cAMP in the cell is a very complex and dynamic process. It involves generation of cAMP by ACs, its diffusion in cytosol and hydrolysis by PDEs (Serezani et al 2008). The kinetics of each mentioned process plays important role in the resulting distribution of cAMP across the cell. Localized mostly on cytoplasmic membrane, when stimulated, ACs are thought to release “clouds” of cAMP that if not sustained move rapidly into cytosol, since diffusion rate of cAMP is in a range between 130 to 700 μm^2 sec^{-1} (Houslay et al 2007). In contrast, regions within the cell with high abundance of PDEs are viewed as cAMP ‘sinks’ that locally drains cAMP (Edwards et al 2011). Another important role of PDEs is hydrolysis of freely diffusing cAMP in the cytosol. Saturation of cytosol with cAMP prevents establishment of any cAMP gradient. Thus by keeping the concentration of cAMP in the cytosol low PDEs confine the formation of cAMP gradients around the source of its generation and channel the signaling around specific signaling modules (Houslay et al 2007). In other words PDEs maintain the favorable signal to noise ratio.

2.2.2.2 Role of scaffold proteins

To provide evidence on how the scaffold protein may influence or form signaling module, role of muscle specific A-kinase anchoring protein (mAKAP) is described here. Importance of proper positioning of PKA by AKAP was shown in skeletal muscle, where ablation of this interaction resulted in inability of PKA to phosphorylate its substrate, L-type Ca^{2+} channels that would otherwise lead to potentiation of the muscle cell and subsequent increase of developed force after stimulus (Johnson et al 1994). Thus AKAPs are thought to direct protein phosphorylation by proper positioning of PKA nearby its corresponding substrate and by ensuring its exposition to the appropriate cAMP gradients or events (Pawson and Scott 1997). This view has been further supported by recently provided evidence that mAKAP ensures the appropriate position of PKA in relation to AC by binding both of them (Kapiloff et al 2009). As seen here on the example of mAKAP, where binding of PKA by mAKAP condition the phosphorylation of L-type Ca^{2+} channels, the topology of crucial enzymes of cAMP signaling pathway has dramatic influence on the speed of signal transduction and even determine the success of the transmission (Johnson et al 1994, Edwards et al 2011).

Regulation of the duration of the signal and it´s termination is further secured by interaction of mAKAP with PDE4D3. As was already mentioned that this interaction is isoform specific thus providing fine tuning of the formed signaling module (Dodge et al 2001). The complex formed by mAKAP, PKA and PDE4D3 is further extended by interaction of PDE4D3 with Epac-1 and subsequently with kinases MEKK, MEK5 and especially ERK5 that is capable of regulating PDE4D3 activity (Dodge-Kafka et al 2005). Dodge-Kafka and colleagues prepared FRET reporter construct simulating the structure of mAKAP-PKA complex. After initial stimulation the PKA kept reporter site phosphorylated thus allowing FRET to occur stably for time period exceeding 15 minutes. However, another construct prepared by the same group that included portion of mAKAP capable of binding PDE4D3 generated localized pulse of FRET signal. The conclusion of this experiment was that the presence of the proteins bound to the complex through PDE4D3, as well as the presence ofPDE4D3 itself, renders the signaling module capable of producing distinct pulses of cAMP or PKA activity (Dodge-Kafka et al 2005).

Implementing organization of the oligomeric structure by AKAP and principle of negative feedback loop involved - a distinct signaling circuit is formed that exploits the spatio-temporal constrains of cAMP distribution in cell in genuine manner that prevents crosstalk among other signaling pathways.

2.2.2.3 Lipids and membranes in cAMP signaling

Organization of biological membranes and role of lipids and proteins in it remains still a controversial topic. The new concept of lipid rafts (membrane microdomains enriched with saturated long faty acid contain phospholipids, cholesterol and proteins with hydrophobic posttranslational modification – eg. Myristoylation, palmitoylation, prenylation, GPI) has evolved from the model of simple fluid mosaic where lipids have just passive structural role. Original mechanistic concept of lipid rafts evolved into a complex model that still uses the term lipid raft, yet the understanding is different (Owen et al 2012). Proteins are according to it clustered on the cell membrane, and in this aspect the evidence is unequivocal (Douglas and Vale2005, Owen et al 2010). The lipid composition varies across the membrane and lipid environment is capable to mediate molecular interactions, however whether the emphasis should be put on the protein-protein or rather on the lipid-driven interactions remains a subject of controversy (Cebecauer et al 2009).

It has been proposed that organizing GPRCs with ACs in membrane microdomains might provide additional way how to compartmentalize cAMP signaling (Houslay et al 2007). Some of the ACs are thought to localize into lipid rafts and caveolae as is the case of AC8 (Kamanetsky et al 2006, Cooper et al 2003). It has been shown recently that AKAP79 interacts with AC8 and regulates its activity (Willoughby et al 2010). Furthermore evidence suggests that this interaction is mediated by lipid environment of plasma membrane, especially because the functional association of AKAP79 with AC8 requires palmitoylation of membrane bound AKAP79 (Delint-Ramirez et al 2011).

The possible role of lipids and plasma membrane in formation of local cAMP gradient points poits out the fact that some of PDEs contain lipid anchors or domains capable of inducible interaction with phospholipids as for example PDE4A1 that contains TAPAS-1 domain (Baillie et al 2002), PDE3 which has been shown to contain transmembrane region

(Shakur et al 2000) or PDE10A2 which membrane localization depends on plamytoylation of its cysteine 11 (Charych et al 2010).

Enzymes competent to form cAMP gradients are known to interact more or less directly with lipids on the plasma membrane and some of these lipids are associated with putative membrane microdomains. The organization of biological membranes is a complicated topic, that has not been solved yet (Owen et al 2012), therefore concepts of membrane spacial microdomain organization is not yet implemented into general paradigm of cAMP signaling. However, despite this, there is evidence, that interactions with lipids or mediated via lipids are important for assembly of cAMP signaling circuits (Delint-Ramirez et al 2001)

2.2.3 Immune system and cAMP signaling

Across the animal kingdom the usage of cAMP is widespread and the physiological responses in which it plays crucial roles are extremely variable. Just to name a few, cAMP plays important role in regulation of blood pressure, cognitive functions as well as in immune system (Beca et al 2011, Serezani et al 2008). It is the immune system that our laboratory is especially interested, thus reviewed here will be the function of cAMP in immune cells.

Innate immune functions of monocytes, macrophages and neutrophils, together simply referred to as phagocytes, is suppressed by elevated levels of intracellular cAMP (Serezani et al 2008). Production of both pro- and anti-inflammatory is modulated by cAMP, however individual cytokines differ in details of the regulation. Both Epac-1 and PKA participate in control of cytokine production, however they might act individually, in concert or against each other (Aronoff et al 2006). For example alveolar and peritoneal macrophages produce tumor necrosis factor α (TNF-α) in response to bacterial lipopolysaccharide. This production is strengthened by addition of Epac-1 agonist, while abolished by PKA agonist, thus illustrating the different effect that stimulation of effector protein by cAMP might have (Aronof et al 2005, Aronoff et al 2006).

Elevated levels of cAMP have been shown to inhibit phagocytosis. Detailed examination of this phenomenon revealed that phagocytosis requires undisturbed function of Epac-1 (Aronoff et al 2005). On the other hand, observation of Makranz and colleagues suggests that the resulting effect of PKA inhibition on phagocytosis depends

largely on the dose of inhibitor (Makranz et al 2006). In general the evidence shows that PKA plays a role in phagocytosis and might be differenty involved in particular cell types (Serezani et al 2008).

Changes in local cAMP concentration during phagocytosis have been imaged recently by implementing FRET based Epac-1 biosensor (Ballinger et al 2010). Transient and localized bursts of cAMP have been observed in place of phagosome formation. This might seem surprising since elevated levels of cAMP have been rather linked to inhibition of phagocytosis (Aronoff et al 2005, Ballinger et al 2010). However, taking the local cAMP grandients into consideration, elevated levels of cAMP concentration may result into saturation of the cytosol by cAMP. High concentration of cAMP is thought to prevent establishment of local gradients and thus disrupt signaling (Houslay et al 2007).

In addition to above mentioned processes, cAMP has been reported to mediate the elimination of phagocytosed microbes via inhibition of formation of the reactive oxygen intermediates (Aronoff et al 2005, Serezani et al 2007).

Apart from its important role in innate immunity, cAMP regulates plethora of processes in cells of adaptive immune system. Chemotaxis of splenocytes has been reported to be abolished after treatment by AC activator forskolin or PDE inhibitor IMBX (Dong et al 2006). Adhesion of T-cell to endothelial cells, that precedes migration into the target tissue, has been shown to be disrupted after elevation of the intracellular cAMP levels (Vang et al 2010). On the other hand, excessive amounts of cAMP are required for the function of naturally occurring T regulatory cells (nTregs) that facilitates the suppression of other T-cells. The regulation of T-cells by nTregs is thought to involve transfer of large amounts of cAMP through gap-junction that the interacting cells form and subsequently by regulation of gene expression as a consequence of cAMP entry (Bodor et al 2012).

Taken together, there are many signaling circuits leading to different cellular response, that implements cAMP as a second messenger (Serezani et al 2008, Bodor et al 2012, Houslay et al 2007). The precise details of their composition, formation and maintenance remain mostly unknown, although there are already some hints about how the specific function and interaction are ensured (Dodge-Kafka et al 2005, Johnson et al 1994). In the

mammalian tissues cAMP plays important role elsewhere, for example in crucial processes of immunity, circulation or cognition (Conti and Beavo 2007).

2.2.4 Adenylate cyclase toxin-hemolysin produced by Bordetella pertussis

Pathogens use various strategies to compete with the host defense mechanisms. Recent host-pathogen interactions are results of long term co-evolution and employ sophisticated molecular mechanisms. One way how pathogens fight on longer distance is secretion of soluble toxins which can alter cellular physiology in many ways, for example interfering with intracellular signalization (Fiser et al 2012). As was mentioned in previous chapters, cAMP is important second messenger and altering its concentration is possible alter the cellular responses or even kill the cell of interest.

Bordetella pertussis, the bacteria responsible for the whooping cough, secretes an adenylate cyclase toxin-hemolysin (CyaA) - a key virulence factor. CyaA is an unusually large, 1706-residue-long, multifunctional secreted protein. It consists of an amino-terminal adenylate cyclase (AC) domain, (400 N-terminal residues) and of an RTX (Repeat in ToXin) cytolysin moiety (about 1306 residues, Vojtova et al 2006). The unique feature of the RTX moiety is ability to insert into membranes and subsequent translocation of the AC domain into cell cytosol (Bumba et al 2010). In the cytosol AC domain binds calmodulin and catalyzes transformation of ATP to cAMP. High enzymatic rate of this reaction dramatically increase intracellular concentration of cAMP, thereby cellular signaling is disrupted subsequently CyaA-catalyzed production of cAMP can promote necrotic cell death or apoptosis Above mentioned function depend on covalent post-translational fatty-acylation of CyaA at internal lysine residues (Vojtova et al 2006).

The capacity of recombinant purified Cya A to bind to the cells, translocate the AC domain into the cell interior and intoxicate the cell via elevated cATP concentration makes for us CyaA as a tempting tool for studying activity of PDE, namely in the context of membrane microdomains, compartmentation of the intracellular signaling and possible interplay between CyaA and PDE8A.

2.3 PDE8A

2.3.1 Gene organization and tissue distribution

In the light of what was said by now many properties of PDE8A will not be surprising and correspond well with the attributes of other PDEs.

Gene coding for PDE8A spans at least 80kbp and consists of 23 exons and 22 introns which are spliced into five variants, labeled as PDE8A 1-5. Of the transcript variants PDE8A1 contains the longest ORF (2490bp) that consists of 22 exons excluding only exon 8, which would eventually disturb PAS domain coded partly by neighboring exons 7 and 9. In addition to exon 8 PDE8A2 excludes also exon 9 and PDE8A3 also exon 7. So far mentioned transcript variants share common start codon, in contrast to PDE8A4, which lacks exon 7 and 8, and PDE8A5 that despite consisting of all 23 exons are translated from alternative start codon located on 9^{th} exon. Thus intriguingly only 4 different proteins are produced. (Wang et al 2001).

Just 11 bp upstream from the transcription site lies a TATA box and further upstream, another 820 bp stretches the CG-rich (70% CG content) promoter of PDE8A capable of harboring transcription factors such as as Oct-R, myogenin and Arnt (Wang et al 2001). The promoter ensures presence of PDE8A1 transcripts in testis, spleen, lymph nodes and various cells of immune systems like Th1, Th2 or activated T-cells where amount of transcripts is reported to rise upon lymphocyte activation (Wang et al 2001, Glavas et al 2001). Transcript of PDE8A2 is found in the same tissues as that of PDE8A1, however the amounts differ. Levels of PDE8A1 are highest in testis, while PDE8A2 is found mostly in spleen, and similarly such differences are found across the tissues where both transcripts were detected (Wang et al 2001)

2.3.2 Features and structure of PDE8A proteins

The PDE8A was recognized simultaneously by two research groups, one identified the human PDE8A (Fisher et al 1998) and the other focused on protein from mouse (Soderling et al 1998). Both isolated proteins were highly cAMP specific with only background cGMP hydrolyzing activity (Fisher et al 1998, Soderling et al 1998). The catalytic domain of isolated PDE8A protein showed only limited degree of sequence identity to the catalytic domains of already known cAMP specific PDEs. While sequence identity between catalytic

domains within the members of PDE gene family is usually more than 85%, the catalytic domain of PDE8A had no more that 40% of sequence identical to any known PDE family at that time. Catalytic domain of PDE8A was found to be most similar to the PDE4 with 38.5% of amino acid sequence identity and least similar to the catalytic domain of PDE6 with sequence identity only 20.2% (Fisher et al 1998). Moreover, PDE8A was not inhibited by most of the inhibitors tested, with dipyramidol as the only exception (Fisher et al 1998, Soderling et al 1998). Based on these data, PDE8A was descriptively named as high affinity cAMP specific and IBMX-insensitive PDE.

Kinetic properties of PDE8A have been determined several times using different PDE8A variants. For full-length mouse PDE8A, K_M of 0.15μM was reported (Soderling et al 1998) and N-terminally truncated human PDE8A displayed value 0.055μM (Fisher et al 1998). In contrast K_M=1.8μM was reported for isolated and refolded PDE8A catalytic domain fragment (Wang et al 2008, Yan et al 2009). This disproportion is probably due to N-terminal negative regulatory effect on enzymatic activity (Wang et al 2008). Catalytic activity of PDE8A1 is dependent on presence of Mg2+ or Mn^{2+} (Fisher et al 1998, Yan et al 2009).

The structure of PDE8A catalytic domain has been determined and revealed what already specific pharmacological profile together with the low degree of sequence identity towards other PDEs indicated. - unique conformation of catalytic pocket (Soderling et al 1998, Wang et al 2008). While in the catalytic pocket of PDE8A1 is a tyrosine residue in position 748, in most other PDEs homologous position is occupied by phenylalanine. Mutation of Tyr748 into phenylalanine renders PDE8A1 susceptibility to various inhibitors, thus implying the crucial role of Tyr748 in PDE8A1 inhibitor selectivity (Wang et al 2008).

Based on the sequence analysis, PDE8A was predicted to contain PAS domain (Soderling et al 1998). Present in many proteins of all kingdoms of life, PAS domains are thought to serve as universal signal sensors and interaction platforms, mediating processes such as diverse ligand binding or protein-protein interaction (Möglich et al 2009). Presence of PAS domain was confirmed in PDE8A1 however splice variant PDE8A2 omits exon 9, that codes for its C-terminal part, resulting into protein with incomplete PAS domain (Wang et al 2001). In PDE8A1 PAS domain mediates binding to IκB that

subsequently results in increased enzymatic activity (Wu et al 2004). Moreover, K_M of cAMP hydrolysis of the PDE8A1 catalytic domain produced separately is 1.8μM compared to K_M of PDE8A1 fragment, that in addition to catalytic domain contains also PAS domain, is 0.28 μM which is approximately 6-fold difference (Wang et al 2008, Yan et al 2009). Such differences indicates important role of PAS domain in regulation of PDE8A1 function (Yan et al 2009)

Apart from PAS domain activity of PDE8A1 is further regulated by PKA phosphorylation at serine 359 (Brown et al 2012). Similarly to PDE4D3, also PDE8A1 is thought to be a part of a feedback loop, where higher cAMP level triggers PKA activation that subsequently phosphorylate PDE8A1 at serine 359 (Brown et al 2012).

Although more potential regulatory regions were proposed for PDE8A, such as REC domain, phosphorylation sites for various protein kinases and putative acylation sites, their functional role has not been assessed yet (Wang et al 2001, Brown et al 2012). Out from these, phosphorylation of PDE8A1 at serine 359 is the only post-translational modification proven and published so far (Brown et al 2012).

2.3.3 Role of PDE8A in physiological processes

Physiological role of PDE8A has not been studied extensively so far, mostly due to absence of specific inhibitor (Vang et al 2010, Brown et al 2012). Although without further details about mechanisms PDE8A was already recognized in diverse physiological processes (Dong et al 2006, Vang et al 2010, Shimizu-Albergine et al 2012, Patrucco et al 2010).

At both transcription and protein level PDE8A is up-regulated in CD4+ T-cells upon their activation by CD3 and CD28 thus suggesting its role in this cell type (Glavas et al 2001). Examination of lymphocytes chemotactic migration toward CXCL12 (stromal cell-derived factor 1) revealed that after activation migration of lymphocytes is degree of inhibition by FSK and IMBX decreases (Dong et al 2006). Moreover migration of lymphocytes is not affected by PDE4-selective inhibitor piclamilast neither by PDE7-selective inhibitor, however is greatly inhibited by dipyramidol (Dong et al 2006). Such pharmacological profile corresponds well with that of PDE8A, which expression levels are increased upon lymphocyte stimulation, thus it was deduced that PDE8A is crucial for chemotactic behavior of lymphocytes (Dong et al 2006, Glavas et al 2001). In addition to

lymphocyte migration PDE8A has been shown to regulate the adhesion of T-cells to endothel via regulation of integrin expression (Vang et al 2010).

High levels of PDE8A transcript were reported from testis (Wang et al 2001) and subsequently PDE8A protein has been found in leydig cells (Vasta et al 2006). In concert with PDE8B and PDE4, PDE8A was found to control steroidogenesis in leydig cells (Vasta et al 2006) as well as in the cells of adrenal gland (Tsai et al 2011). In addition PDE8A has been reported to regulate potentiation of contraction of ventricular myocytes (Patrucco et al 2010), however no systematic long term research on the physiological roles of PDE8A is conducted, most probably due to the lack of selective inhibitor (Brown et al 2012, Vang et al 2010). Recently a PDE8 specific inhibitor has been reported (Vang et al 2010, Tsai et al 2011), however its implementation into research of PDE8 is still limited.

3 Materials and methods

3.1 Material

3.1.1 Laboratory machines

autoclave PS20A (Chirana), CCD camera Exwave HAD (Sony), centrifuge Universal 16R (Hettich Zentrifugen), centrifuge Universal 32R (Hettich Zentrifugen), centrifuge K26D, benchtop centrifuge Minispin Plus (Eppendorf), thermal cycler PTC100 (MJ Research), thermal cycler XP (Bioer), glass electrode pH meter AD1030 (Adwa), thermoblock Thermomixer comfort (Eppendorf), custom made electrophoretic set (J. Macha), inverted microscope IX-71 (Olympus), inverted mikroscope IX-81 Cell'R' s equipped with fluorescent filters U-M3DAFITR (Olympus), spectrophotometer UV-1601 (Shimadzu), trans-illuminator TCP-20MC (Vilber Lourmat), set of mechanic pipettes EpResearch pipet (Eppendorf), Nanodrop ND-1000 (Thermo scientific), cytometer LSRII (BD), Laminar flow biosafety cabinet EF/B (Clean Air) confocal microscope Leica TCS SP2 (Leica) equipped for live cell imaging, shaking incubator NB-205 (N-Biotek), orbital shaker incubator (Neq), DC power source Power Station 300 (Labnet), spectrophotometer UV-1601 (Shimadzu), weighting scale ABC plus 600H (ADAM Equipment), vortex MS1 minishaker (IKA),

3.1.2 Chemicals and reagents

10x Long PCR Buffer with $MgCl_2$ (MBI Fermentas), 10x High fidelity PCR Buffer with $MgCl_2$ (MBI Fermentas), 10x PfuUltra II reaction Buffer (Stratagene), 10mM $MgCl_2$ (MBI Fermentas), β2-merkaptoethanol (Sigma), Annexin V-DY-647 (Exbio) agarose for electrophoresis (Invitrogen), ampicilin (Sigma), bromphenol blue (Sigma), $CaCl_2$ (Sigma), 4',6-diamidino-2-phenylindole (DAPI; Sigma), agarosa pro elektroforesu (Invitrogen), ampicilin (Sigma), D-MEM (Gibco), RPMI 1640 (Gibco) deoxyribonucleotides (dNTP, MBI Fermentas), ethylenediaminetetraacetic acid (EDTA, Sigma), calf intestine alkaline phosphatase (CIAP, MBI Fermentas), T4 DNA ligase (MBI Fermentas), phalloidin-AlexaFluor 568 conjugate (Molecular probes), phenol (Lachema), fetal bovine serum (FBS, Gibco), formaldehyde (Sigma), geneticin (Gibco), glukose (Lachema), glutamine (SEVAPHARMA), chloroform (Lachema), kanamycin (Sigma), KH_2PO_4 (Lachema), Zyppy plasmid miniprep II kit Zymmo research), Zymoclean gel DNA recovery kit (Zymmo research), cover glass slides round 8mm (Hirschmann), Lipofectamine 2000 (Invitrogen), SOC medium (Invitrogen), methanol (Lachema), $MgCl_2$ (Sigma), Urea (Lachema), Mowiol 4-88(Calbiochem), Na2HPO4.12H2O (Lachema), NaCl (Lachema), NaN3 (Sigma), NH4Cl (Lachema), Nuclease free H2O (MBI Fermentas), Nutrient agar (OXOID), Glass bottom petri dishes for live cell imaging (Mat Tech), Disposable plastic Pasteur pipettes and pipette tips (Nunc, Eppendorf), Disposable plastic plates and flasks for cell culture (Nunc), glass slides for microscopy 76x26 mm (Hirschmann), primers and olignucleotides (Sigma), DMSO solution (Sigma), buffers for restriction endonucleases (MBI Fermentas), restriction endonucleases (MBI Fermentas), sterile Trypsin-EDTA, 10x (Sigma), LA DNA polymerase (Top-Bio), PfuUltra II Fusion HS DNA polymeraqse (Stratagene), tris(hydroxymethyl)aminomethan (Tris, Sigma), Tryptose Phosphate Broth (OXOID), Triton X-100 (Sigma), GeneRuler™ DNA Ladder Mix, 100-10,000 bp (MBI Fermentas), Ethidium

bromide homodimer (Molecular probes), Ethidium bromide (Sigma), H_3BO_3 (Lachema), cyclase toxin from Bordetella pertussis (cya A, kindly provided by Peter Šebo), Isopropyl β-D-1-thiogalactopyranoside IPTG (Sigma),
5-bromo-4-chloro-indolyl-β-D-galactopyranoside (X-gal, Sigma)

3.1.3 Vectors

pmCit-N3 was provided by Lukáš Falteisek as vector carrying PDE8A1(N) constructs. Vector is designed for expression of proteins with citrine fluorescent tag fused to their C-terminus in mammalian cells. It was derived from pEGFP N3 (Clontech) by exchange of region coding for fluorescent tag so that citrine replaced GFP in the original vector. Restriction sites BamHI and BsrGI were used for this exchange. Other features of the original vector were retained.

pGem-T easy was obtained from Promega (Promega Corporation) as a part of pGem-T Easy Vector System for cloning of PCR products. It is supplied linearized by EcoRV with added T overhangs and allows blue/white screening of recombinants.

3.1.3.1 Plasmids for analysis of alternative splicing

PDE8A_c1_2010, PDE8A_c8_2010 and PDE8A_D_tupo used for analysis of alternative splicing of PDE8A were left overs form unsuccessful attempts to clone PDE8A1.

3.1.4 Solutions

If not stated otherwise, solutions were kept in refrigerator at room temperature on light.

EDTA 2%
4g EDTA dissolved in 100 distilled H_2O; alkaline pH adjusted by 6 ml of 10M NaOH to facilitate dissolving of EDTA; pH adjusted back to 7.2 by 4 ml of 6M HCL; water added to final volume 200 ml

Mowiol with DAPI
20% (w/v) glycerol; 10% (w/v) Mowiol 4-88; 0.1 M Tris.HCl; pH 8.5; DAPI 1µg/50ml, stored in dark at 4°C.

Buffer TUC
50mM tris; 8M urea; 0.2 mM CaCl2; stored at -20°C

10x PBS
79 g NaCl; 1,1 g KCl; 29 g $Na_2HPO_4.12H_2O$; 3,1 g KH_2PO_4; distilled water added till final volume 1 l

Agarose gel electrophoresis

TBE buffer
89 mM Tris.HCl; 89 H_3BO_3 (Lachema); 2 mM EDTA; pH 8.0

Sample buffer
50% glycerol; 0.13 M EDTA; 0.12% bromphenol blue; pH 8.0

Cultivation of *E. coli*

TPB
29.5 g/l Tryptose Phosphate Broth; sterilized at 121°C for 15 min in autoclave; skladováno při 4°C

Nutrient agar
28 g/l Nutrient Agar; sterilized at 121°C for 15 min in autoclave; antibiotics added after medium have cooled to 40°C

1M $MgCl_2$
20.3 g MgCl2 . $6H_2O$/100 ml

1M $CaCl_2$
11.1 g $CaCl_2$/10 or 14.7 g $CaCl_2$. 2 H_2O/100 ml

Buffer 0.1M $CaCl_2$ + 14%glycerol 50 ml
80% glycerol 8.25 ml; 1M $CaCl_2$ 5 ml; H_2O added till total volume 50 ml

10x PBS
79 g NaCl; 1,1 g KCl; 29 g $Na_2HPO_4.12H_2O$; 3,1 g KH_2PO_4; distilled water added till final volume 1 l

Cell cultures

Water for cell cultures ("TK H_2O")
Deionized water was sterilized at 121°C for 20 minutes in autoclaving machine

D-MEM
90% (v/v) D-MEM; 10% (v/v) FBS; 40 µg/ml gentamycin; 0,25 mg/ml glutamine; prepared sterile; storage at 4°C

RPMI 1640
90% (v/v) RPMI 1640; 10% (v/v) FBS; 40 µg/ml gentamycin; 0,25 mg/ml glutamine, β-merkaptoethanol 0,05 mM; prepared sterile; storage at 4°C

PBS TK
10x PBS (79 g NaCl; 1.1 g KCl; 29 g $Na_2HPO_4.12H_2O$; 3.1 g KH_2PO_4) TK H_2O added till final volume 1l; filtered and sterilized at 121°C for 20 minutes in autoclaving machine; diluted 10x befor use by TK H_2O

EDTA 0.02% for cell culture application
2% EDTA filtered and diluted 100x by TK PBS

10x Trypsin EDTA for cell culture application (Sigma)
5g porcine trypsin, 2g EDTA, 0,9% NaCl do 100 ml

3.1.5 Laboratory organisms used

3.1.5.1 E. coli strain TOP10 (Invitrogen)

F- mcrA Δ(mrr-hsdRMS-mcrBC) φ80lacZΔM15 ΔlacX74 deoR nupG recA1 araD139 Δ(ara-leu)7697 galU galK rpsL(Str^R) endA1 λ^-
(designed for cloning, slelcted endonucleases eliminated, suitable for amplification of large plasmids, blue/white screening – lac operon deleted and for α- complementation partly deleted lacZ introduced on φ80

3.1.5.2 Raw 264.7 cell line

Mouse leukaemic macrophage cell line established from tumor induced by Abelson murine leukemia virus. Morphology of the cells is similar to monocytes and macrophages. Cells are capable of pinocytosis as well as of phagocytosis (ATCC website). Cell line was kindly provided by P. Šebo.

3.1.5.3 CHO cd11 cell line

Adherent cell line with epithelial morphology established from Chinese hamster ovary cells. CHO cd11 was derived from the original line by establishing stable expression cd11, an α component of various integrins that is present on macrophages and utilized by cya A for entry into cells (L. Bumba personal communication). Cell line was kindly provided by L. Bumba.

3.2 Methods

3.2.1 Site directed mutagenesis

3.2.1.1 Eliminating mutations in PDE8A1 constructs

Primers covering the single point mutations (Tab. were designed so that the resulting sequence after amplification would match PDE8A1 (GI:47132535).

primer designation	primer sequence	T_m
8a_opr_I	GTTTAAGTGTACAGTTACCAAGGAGGCTCAGGCTGTCCTTGCCTGTTTCCTGGACAAA	80°C*
8a_opr_II	ATGCATGAATTTATAGTATCGAGCAAGTCAGCCTTTTTTTCATTTATAGG	75°C*
8a mAFP N3 R	GGATCCTTCAGGAGGTGGTCGGAGGTT	65/70°C

Tab 3.1 List of primers used for site directed mutagenesis in order to eliminate sequence conflicts between available PDE8A1 and PDE8A1 reference sequence (GI:47132535); Highlighted in yellow are sites of mutagenesis that reference sequence; Underlined are restriction sites BsrGI; NsiI and BamHI in primers 8a_opr_I; 8a_oprII and 8a mAFP N3 R respectively; * indicated are melting temperatures for perfectly matching oligonucleotide; Tm are calculated using web based program Oligonucleotide properties calculator (http://www.basic.northwestern.edu/biotools/oligocalc.html)

Reaction mixture consisted of:

10x LA polymerase buffer	5µl
primer F (25 µM)	2µl
primer R (25 µM)	2 µl
dNTP (10 mM)	1 µl
template DNA	60 ng
LA DNA polymerase (5U/µl)	0.5µl
H_2O	38,5 µl

PCR was performed in 32 cycles with initial denaturation at 94°C for five minutes. Cycle parameters were: denaturation 94°C 20s; annealing 65°C 20s; elongation 68°C 1:20 (m:s). Products subsequently underwent agarose gel electrophoresis. Bend of corresponding length was extracted and cloned into pGem-T easy.

3.2.1.2 Preparation of catalytically inactive PDE8A1

Perry and coworkers (Perry et al 2002) successfully generated inactivated PDE4D5 protein by making single mutation Asp^{556} to Ala (D556A) in the catalytic site. Catalytic site is

conserved among PDEs so that corresponding residue was identified in PDE8A1 protein coding sequence (Fig. 3.1).

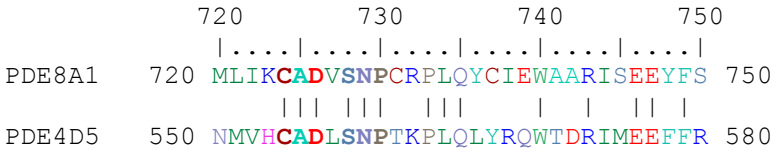

Fig 3.1 Sequence alignment of catalytic domains of PDE8A1 and PDE4D5; Note the aspartate residue (at 726 in PDE8A and 556 in PDE4D that is important in ensuring binding of divalent cation and thus preserve functionality of PDEs

The position of identified residue verified by examination of protein 3D structures available for catalytic domains PDE4D5 and PDE8A.
Both strands of PDE8a_H2RB plasmid were amplified from primers 8aINA F and 8aINA R (Tab. 3.2) designed to introduce mutation of adenine at 2177 to cytosine (2177A->C; Fig. 3.2) in 12 cycle PCR by *PfuUltra* II Fusion HS DNA polymerase. Reaction mixture and conditions were as summarized in table 3.3 and 3.4 respectively.

PDE8A1

```
2161  CTG ATT AAA TGT GCT GAT GTG TCC AAT CCC TGC CGA CCC CTG CAG   2205
721   Leu Ile Lys Cys Ala Asp Val Ser Asn Pro Cys Arg Pro Leu Gln   735
```

PDE8A1_inactivated

```
2161  CTG ATT AAA TGT GCT GCT GTG TCC AAT CCC TGC CGA CCC CTG CAG   2205
721   Leu Ile Lys Cys Ala Ala Val Ser Asn Pro Cys Arg Pro Leu Gln   735
```

Fig. 3.2 Nucleotide sequence and its translation of PDE8A1 catalytic domain, before (up) and after site directed mutagenesis; Frame marks the target codon

primer designation	primer sequence	T_m
8aINA F	GCTGATTAAATGTGCTGCTGTGTCCAATCCCTGCC	75°C
8aINA R	GGCAGGGATTGGACACAGCAGCACATTTAATCAGC	75°C

Tab. 3.2 Primers for A2177C site directed mutagenesis

10x *PfuUltra* II reaction buffer	5µl
dNTP (10mM)	1µl
DNA template	30-40ng
Primer 8aINA F	125ng
Primer 8aINA R	125ng
PfuUltra II Fusion HS DNA polymerase	1µl
H_2O	up to 50µl final volume

Tab. 3.3 Content of PCR mixture for A2177C site directed mutagenesis

	Initial denaturation	94°C	5:00
12 cycles	Denaturation	94°C	0:20
	Annealing	55°C	1:00
	Elongation	72°C	2:10
	Final elongation	72°C	3:00

Tab. 3.4 Parameters of PCR run for A2177C site directed mutagenesis.

After PCR run mixture was incubated for four hours with methylation sensitive restriction endonuclease DpnI that digest the parental DNA template, but preserve the newly synthetized DNA. Distinction is based on the methylated state of the DNA isolated from E. coli, while strands synthetized by *PfuUltra* II Fusion HS DNA polymerase in the PCR run are not. Chemocompetent bacteria were transformed by the resulting mixture.
Since full-length PDE8A1 constructs contained CG rich segment, that would disturbed PCR amplification of the whole plasmid, PDE8a_H2RB that lacked this segment was used as a template. The whole sequence coding catalytically inactivated PDE8A was assembled afterwards by means of cloning and restriction enzymes.

3.2.2 Transformation of chemocompetent bacteria

Chemocompetent cells of *E. coli* strain were stored at -80°C. Before use the cell suspension was briefly thawed on ice. Either 0.3µl of plasmid DNA or 3µl of ligation mixture were added to 40µl of cell suspension and incubated on ice for 20 minutes. Cells were heat-shocked by incubation for 40s at 42°C and then cooled on ice for 2 minutes. Afterwards 200µl of SOC medium were added and bacteria were incubated in thermoblock at 37°C and constant shaking (1200 rpm) for one hour. The suspension was plated on nutrient agar in petri dishes with appropriate antibiotics and incubated over night at 37°C.

3.2.3 Plasmid isolation

For routine needs Zippy Plasmid miniprep kit was used according to protocol provided by manufacturer. For this purpose bacterial cultures were grown in 3 ml of liquid medium on nutrient agar plate covering quarter or whole surface, depending on the amount of DNA needed. Bacterial cultures were grown in the presence of appropriate antibiotic.
In case of full-length PDE8A1 constructs large amounts of DNA were need. For this purpose, Qiagen Maxi prep kit was used to isolate plasmid DNA from 0.5l of the culture. Procedure was performed according to protocol provided by manufacturer.

3.2.4 Restriction digests

3.2.4.1 Single digestion

For single digestion buffer where desired restriction endonuclease is fully active was chosen. Reaction mixture composed of:

Plasmid DNA	0.5-2µg
10x concentrated buffer	1µl
restriction endonuclease (10U/µl)	0.5µl
H_2O	up to total volume 10µl

Mixture was incubated at 37°C for an hour.

3.2.4.2 Double digestion

Buffer where both desired restriction endonucleases were sufficiently active was chosen. Reaction mixture composed of:

Plasmid DNA	0.5-2µg
10x concentrated buffer	1µl*
restriction endonuclease (10U/µl)	0.5µl
restriction endonuclease (10U/µl)	0.5µl
H_2O	up to total volume 10µl

*In some cases use of 2x tango buffer was preferred thus 2µl were used instead

Mixture was incubated 37°C for an hour.

3.2.4.3 Scaling and analysis of DNA digestions

In case of preparative digestion higher concentrations of DNA fragment were desired, thus higher amount of plasmid DNA was required in the reaction, what was especially important when the fragment of interest represented only a small portion of the plasmid. While performing digestion in >30µl ratios of DNA and buffer were conserved, while only half of the enzyme was used. As compensation mixture was incubated for two hours instead of one.

To fragments, intended to serve as a vector in subsequent ligation, calf intestine alkaline phosphatase (CIAP) was added.

Samples were subsequently run on agarose gel to separate individual fragments.

3.2.5 Agarose gel electrophoresis

Electrophoresis was performed at standard condition in 1% (w/v) agarose gel with 1 µg/ml

ethidium bromide in TBE under stable voltage 17 V per cm of gel length. Before loading bromphenol blue was added to the sample in 1:5 (Bromphenol blue:Sample) ratio. For short DNA fragments (<300pb) thicker 2% agarose (w/v) gel was used. Gene Ruler DNA ladder mix was loaded beside samples. After the run gels where examined on UV-transluminator and pictures were taken by CCD camera Exwave HAD with “quick photo micro” software.

3.2.6 Extraction of DNA fragments from agarose gel

DNA fragments were separated on agarose gel electrophoresis. Upon examination on UV transluminator, fragments of desired length were excised by scalpel at maximum possible speed to minimize DNA damage by UV light and transferred to test tube. DNA was extracted by Zymoclean^{TM} gel DNA recovery kit (Zymmo research) according to protocol provided by the manufacturer.

3.2.7 Ligation of DNA

Vectors and fragments obtained from the follow-up steps of restriction, electrophoresis and DNA extraction were ligated together. Ligation mixture composed of

10x T4 DNA ligase buffer	1µl
Linearized vector	100-500ng
insert	in 1:1 ratio to vector
T4 DNA ligase (5 Weiss U/µl)	0,5 µl

and was incubated at room temperature for an hour. The ligation mixture was then used to transform TOP10 chemocompetent bacteria, a strain of *E. coli*. The vector insert molar ratio was approximately kept by putting approximately same amount of plasmid DNA already into the DNA digestion. If ligation failed procedure was repeated with several altered concentrations and ratios of both vector and insert.

3.2.8 Sequence determination of PDE8A1

Primers used for sequencing are listed in the table and their distribution on PDE8A1 coding sequence is shown in figure. Sequence was determined in Laboratory of DNA sequencing at Faculty of Science (Charles University in Prague). After every step during preparation of PDE8A1 clones that gave positive results on restriction analysis were sequenced.

primer designation	primer sequence	T_m
8aN_F	AATCTCGAGATGGGCTGTGCCCCGA	72°C *
8aN_R	AATGGATCCTTCTTGCCGCTGCCG	64°C
8aIM_1_R	CTCGAGTTATGGGACATCATCAAGGGAG	60 °C
8aIM_2_F	GGATCCACTGAGTTATATTCACCACAGTT	59 °C
8aIM_3_F	GGATCCATCAACAAACCCTTGGCAAC	59 °C

Tab.X List of primers used for sequencing of PDE8A1 constructs. Primers were originally used for cloning of segments of PDE8A1 thus they contain restriction sites that do not hybridize with PDE8A1 coding sequence. Melting temperatures provided include this into consideration. Exception to this 8aN_F (T_m denoted by star) where underlined restriction site has been incorporated into PDE8A1 constructs. Letters F or R in the suffix of the primer name iondicate primer orientation

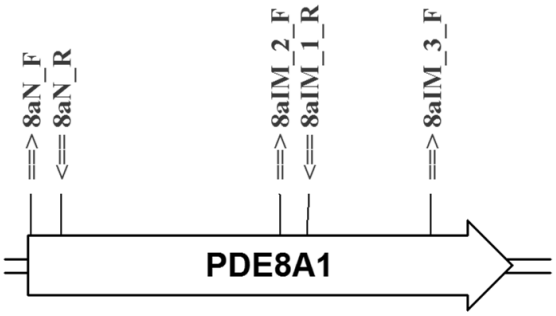

Fig. 3.3 Distribution of sequencing primers across the PDE8A1 gene. Positions are proportional. Downwards arrows indicate primer orientation toward 5'-end of CDS.

3.2.9 Cell cultures

3.2.9.1 Cultivation conditions

All cell lines used were kept in stable 5% CO2 atmosphere at 37°C. CHO cd11 cells were grown in D-MEM medium, while RAW264.7 cells were kept in RPMI 1640, both media contained 10% fetal bovine serum.

3.2.9.2 Passages of cell lines

From adherent cell line CHO cd11 cultivation medium was removed, afterwards were cells rinsed by PBS and subsequently covered by minimal volume of PBS containing 0.5% trypsin and 2.0% EDTA. After brief, approximately 5 minute long, incubation they were flushed from the cultivation surface by the stream of the passaging solution and resuspended. Medium was added to 10% of the cell suspension for further cultivation.
Similarly cultivation medium was removed from RAW264.7 cells, then 3 gentle rinses by PBS followed and afterwards, since adhesion of RAW264.7 to cultivation substrate is very weak, cells were resuspended by vigorous streaming of minimal volume of PBS over them. In cultivation flask 10% of cell suspension was kept and medium was added. RAW264.7 required fresh medium twice a week.

3.2.9.3 Transformation of cell lines by lipofectamine transfection reagent

Freshly passaged cell suspension was distributed evenly into wells of experimental plate. Amounts were approximately adjusted so that the next day would cells reach 90% confluency.
Transformation of the cells was done by Lipofectamine 2000 according to protocol provided by the manufacturer. Amounts of reagents and DNA used for transfection were adjusted to volumes of cultivation media and size of the well according to scale provided in the protocol. For one well of 24-well plate transfecting particles were prepared as follows, first 2µl of lipofectamine reagent were diluted in 50 µl of medium without serum and antibiotics, then in the same volume of medium 0.8 µg of DNA used for transfection was diluted. After brief incubation diluted transfection reagent and DNA were mixed together and incubated for 25 minutes, then added to cultivation well.
To prevent toxic effect of the reagent on cell viability, medium was exchanged 8 hours after transfection. Cell culture was screened for transfected cells 8-24 hours afterwards.

3.2.9.4 Preparing cell lines expressing variants of PDE8a for microscopy

Cells were plated into cultivation wells containing microscopic glass slides one day before transfection and left to grow up to 90% of confluency. Transfection procedure was performed as described in previous clause. Mostly 24-well plates were used. If used, transferrin-alexa594 of final concentration 50µg/ml or mitotracker-alexa594 was added to cultivated cells 2 hours before fixation.

3.2.9.5 Fixation and preparation of specimen for microscopy

For fixation medium was removed and 4% formaldehyde was added to cells for 20 minutes without prior rinse. After fixation cells were rendered permeable by incubation in 0.5% triton X-100 in PBS for 1 minute and rinsed with PBS for 3 times. If phalloidin-allexa594 was used to stain actin cytoskeleton, it was added after this step (0.2U per 1.9 cm^2 of cultivation surface).

Glass slides were then removed from cultivation plate and fixed on microscopic slide with drop of mowiol-dapi. Specimens were examined by Cell'R' microscopic system.

3.2.9.6 Preparation of samples for flow cytometry

Supernatants were collected from cultivation wells that were subsequently gently rinsed by PBS for 3 times. Cells were incubated in minimal volume of 0.02% sterile EDTA for 15 minutes to weaken their adherence to cultivation surface. Cells were resuspended and kept on ice before further processing.

If larger samples were used, the collected cell suspensions were centrifuged for 4 minutes at 250g at in pre cooled centrifuge. Supernatant was discarded and cells were resuspended in approximately 200µl of 0.02% EDTA and analyzed subsequently.

For staining by annexin V collected samples were centrifuged for 4 minutes at 250g in cooled centrifuge. Supernatant was discarded and cells were resuspended in annexin V-binding buffer and centrifuged again, this step was added in order to ensure sufficient Ca^{2+} for annexin binding, that that was depleted by EDTA. Pellet was resuspended in annexin binding buffer with added annexin V and incubated for 20 minutes at room temperature.

Cells were kept on ice and directly before analysis on LSR II (BD) either 5µl of DAPI(100µg/ml) or 3µl of EtBr (2mM) were added to cell suspension.

3.2.9.7 Treatment of cell cultures by cya A

Concentrated Cya A was kept frozen at -20°C in TUC buffer. Before addition to cells it was thawed swiftly to prevent precipitation and diluted in TUC buffer. Cells were treated by cya A while in D-MEM medium containing 100x diluted TUC buffer. To ensure similar conditions control cells were treated with 100x diluted TUC as well.

Length of incubation as well as concentration of Cya A is indicated in particular experiment.

3.2.10 Confocal microscopy of living cells

Cells were plated on 36mm glass bottom dish in minimal volume one day before transfection. Transfection procedure was performed as described in 1.7.9.3 with scaling according to surface covered by cells ($8cm^2$). For transfection approximately equimolar mixture of PDE8A1(WT)-mCit and PDE8A(N-WT)-mStraw was used. Medium was exchange 8 hours after transfection and cell culture was screened for cells expressing fluorescent.

Cells were imaged on Leica TCS SP2 confocal microscope while maintaining stable 5%CO_2 atmosphere and temperature at 37°C in the chamber for live cell imaging.

3.2.11 Flow cytometry

Flow cytometer was calibrated for the cell line used before every experiment. Scaters were adjusted to detected at least 95% of all events thus providing good resolution. FSC scaling area was adjusted.

Viability of cells was evaluated by flow cytometry. Cells stained positive for DAPI, or EtBr were considered dead and cells stained by Annexin V were undergoing apoptosis.

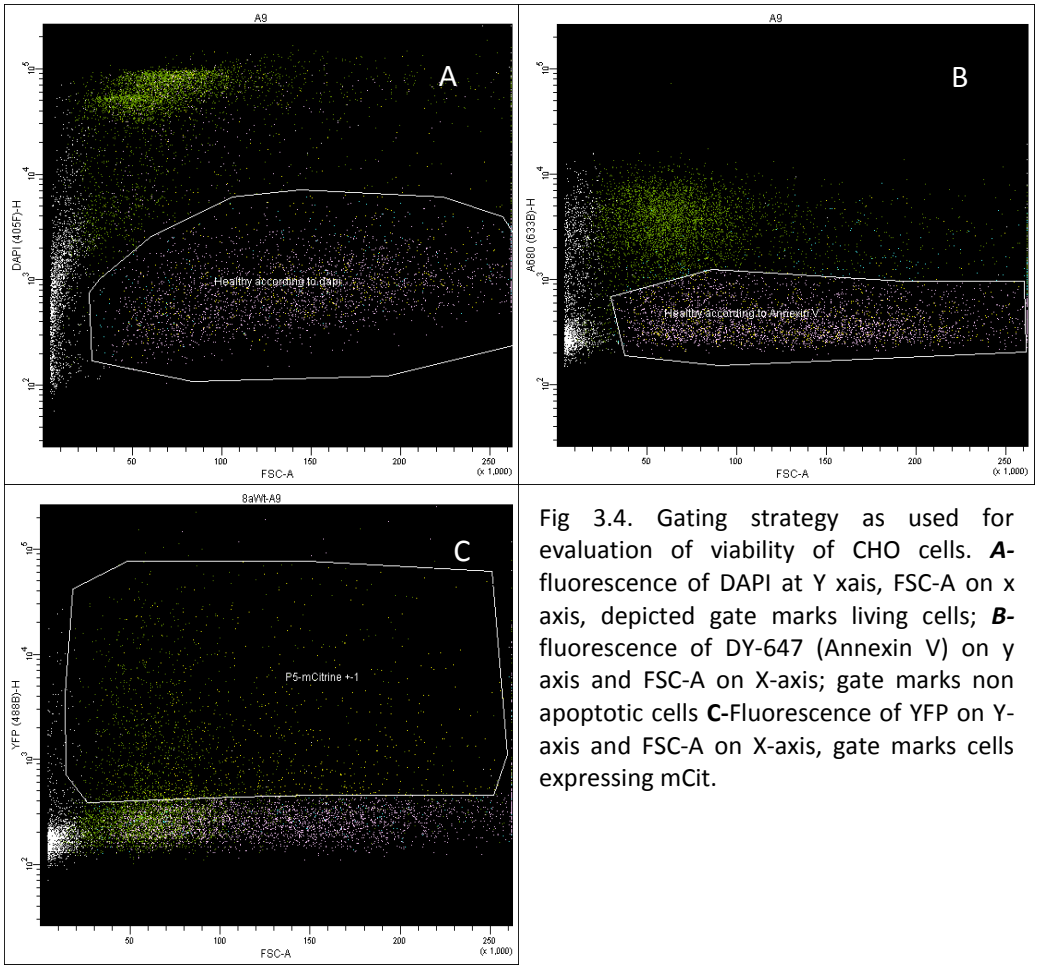

Fig 3.4. Gating strategy as used for evaluation of viability of CHO cells. ***A***- fluorescence of DAPI at Y xais, FSC-A on x axis, depicted gate marks living cells; ***B***- fluorescence of DY-647 (Annexin V) on y axis and FSC-A on X-axis; gate marks non apoptotic cells **C**-Fluorescence of YFP on Y-axis and FSC-A on X-axis, gate marks cells expressing mCit.

4 Results

Membrane biology is one of the most prominent research interests in the laboratory of immunology, where this diploma thesis has been elaborated. On the basis of bioinformatical search PDE8A1 was identified as one protein with putative membrane localization similar to Src kinases associated with lipid rafts that were under investigation by our group (Falteisek 2008). In addition there was evidence that PDE8A plays role in activated T-lymphocytes (Glavas et al 2001) so decision to continue research on PDE8A was taken (Falteisek 2008).

First step was to obtain full-length PDE8A coding sequence.

4.1 Construction of PDE8A-mCit and its variants with modified N-terminus

Due to the research previously conducted in our laboratory (Falteisek 2008) DNA-constructs containing PDE8A1 coding sequence were already available. However detailed sequencing revealed that none of the clones contained sequence identical to the canonical PDE8A1 (GI:47132535). The content of available clones was examined in detail subsequently strategy to obtain PDE8A1 coding sequence was built.

4.1.1 Alternative splicing of PDE8A

Gene organization of PDE8A has been reported and exon/intron boundaries are known (Wang et al 2001). Brief sequencing of three most prospective of available clones suggested that they carried cDNA of alternatively splice PDE8A transcripts. Analysis of exon composition of the clones concerned revealed that they were indeed splice variants of PDE8A transcript (Tab 4.1). In addition to exon 8, that is not present also in PDE8A1 isoform, exons 3,4 and 5 were missing in the PDE8A_c1_2010. In contrast, all the exons, that PDE8A1 consists of, were present in PDE8A_D_tupo, however there was additional segment between exon 3 and 4. Similarly PDE8A_c8_2010 contained additional sequence region between exons 18 and 19, however lacked exons 4, 5, 7 and 9 that are present in PDE8A1. The additional sequence segments found fit well on already known exon-intron

boundaries. Newly identified segments were found in known retained introns of PDE8A protein coding transcripts, however in introns they were surrounded by sequences different to those we have found in our clones. This indicates existence of yet unknown splicing sites on borders of the newly identified segments.

	1	2	3	N	4	5	6	7	8	9	10	11	12	13	14	15	16	17	18	N	19	20	21	22	23
PDE8A_c1_2010	x	x	-	-	-	-	x	x	-	x	x	x	x	x	x	x	x	x	x	-	x	x	x	x	x
PDE8A_c8_2010	x	x	x	-	-	-	x	-	-	-	X	x	x	x	x	x	x	x	x	!	x	x	x	x	x
PDE8A_D_tupo	x	x	x	!	x	x	x	x	-	x	x	x	x	x	x	x	x	x	x	-	x	x	x	x	x

Tab 4.1 Exon composition of selected clones. Numbers (1-23) indicate recognized exons; N indicates segments not listed nor numbered as exon in Ensembl database; Absence of exon is marked as – and its presence as X. Segments previously identified as introns are indicated with !; N indicates

4.1.2 1st mutagenesis

Cloning of PDE8A has been proven complicated (Falteisek 2008, Fisher et al 1998). However since constructs with incomplete or mutated PDE8A were already available another way to obtain PDE8A1 coding sequence was to either combine them or to repair the mutations present there by site directed mutagenesis, so that the resulting sequence would match canonical PDE8A1 (GI:47132535).

Construct PDE8A_mCit_D, already present at our laboratory (heritage from Lukáš Falteisek), contained coding sequence for whole PDE8A1 protein tagged with citrine, however it carried point mutations 324A->G, 346G->C, 348C->T and 358T->C. Although mutation of A to G at position 324 would not change amino acid in resulting protein, the mutation of G to T at 346 in concert with mutation C to T at 348 would change valine at position 116 to phenylalanine. Moreover mutation of T to C at 358 would result in replacement of original Phe120 by leucine. Mutation of nucleotides and their consequences are depicted in table 4.2

position	Change in nucleotide sequence	Cosequences in AA sequence
324	A->G	-
346	G->T	V116F
348	C->T	
358	T->C	F120L

Tab 4.2 Overview of mutations in coding sequence of PDE8A1 as present in PDE8A_mCit_D and their consequences in amino acid sequence of encoded protein

Otherwise PDE8A_mCit_D was considered to be complete and correct. Primer 8a_opr_I was designed to repair above mentioned mutations, and together with primer PDE8A amAFP N3 R was used to perform PCR (see chapter … and the amplified segment was cloned into pGEM-T easy vector according to protocol provided by manufacturer. The resulting ligation mixture was used to transform TOP-10 chemocompetent *E. coli* cells and screened for successful ligation the next day. The result of this procedure was DNA construct termed PDE8A_oprI8-pGEM which contained segment of PDE8a (nt 324-2487) without mutations 324A->G, 346G->T, 348 C->T and 358T->C.

The only was how to incorporate the repaired segment back into PDE8A1 coding sequence was through the BsrGI site however this was disrupted in PDE8a_mCit_D. Furthermore in PDE8A1 sequence there was another BsrGI restriction at nt 1857, splitting the assembly of PDE8A1 into more steps. So it was necessary to assemble PDE8A1 coding sequence piece by piece. The next step was to transfer nt 1857-2487 into PDE8A_c8_2010, that was planned to be followed by addition of segment between two BsrGI sites (nt 324-1857) and subsequently by addition of 5'portion of the gene that encoded the very N-terminus. The first step was successful indeed and resulted in construct PDE8A_oprI8_R14. However meanwhile the first step was finished, sequence of the 1534bp long segment between two BsrGI sties was determined and revealed another five point mutations that were present both in the template PDE8a_mCit_D as well as in PDE8a_opr-I8. One of those mutations, 806A->G, would eventually result in altered protein sequence, where lysine would be replaced by arginine (269K->R).

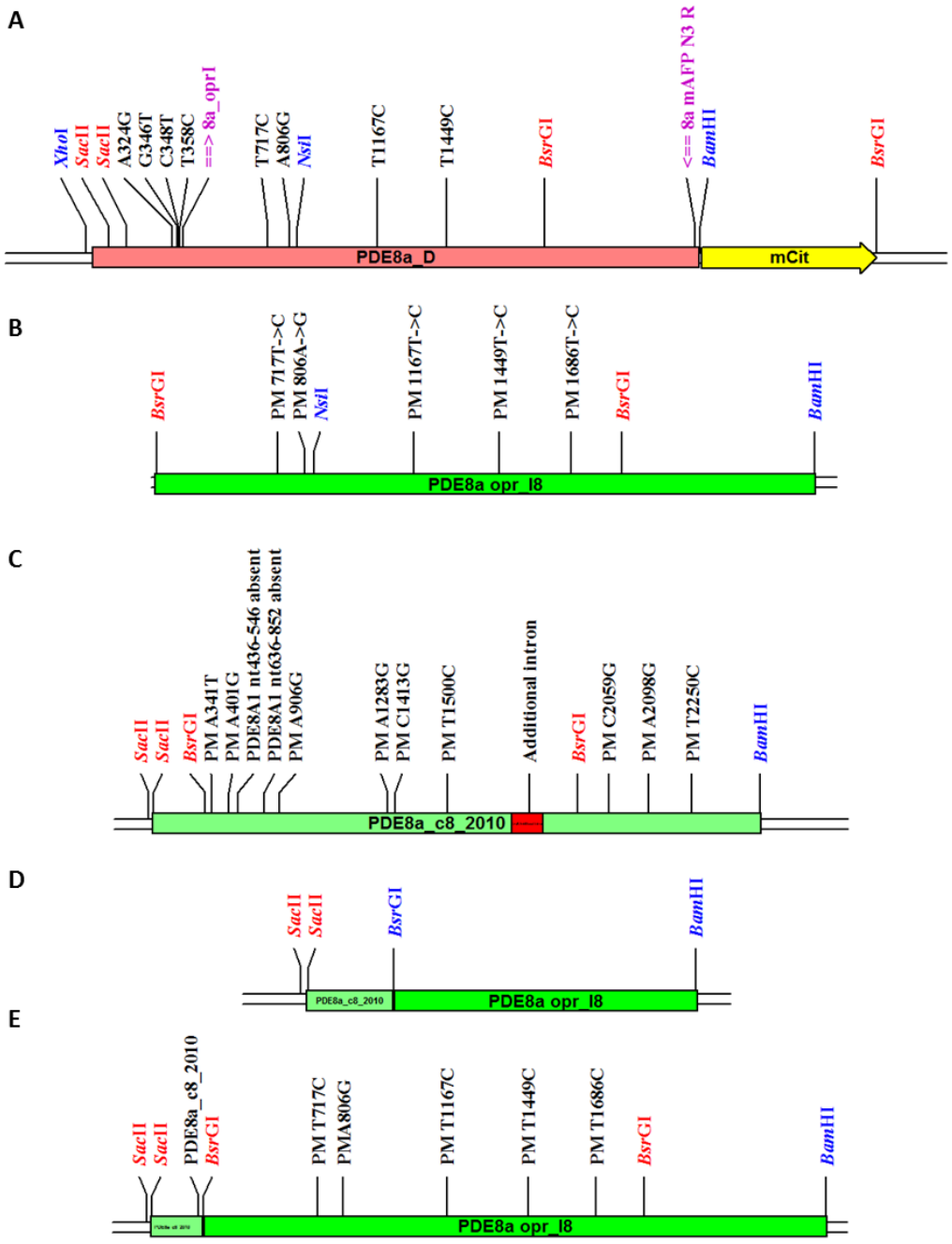

Fig3.1 Schematic depiction of important features of PDE8A constructs. Depicted are point mutations (PM) as well as restriction sites important for cloning of PDE8A1 (SacII, BsrGI and BamHI); ***A***-PDE8A_mCit_D construct with primers used for site-directed mutagenesis: 8a_oprI and 8a mAFP N3; ***B***-PDE8A_oprI8-pGem with cloned product from mutagenic PCR; ***C***-PDE8A_c8_2010 that was used as a donor of nt 135-323 segment; ***D***-PDE8A_oprI8_R14 was generated by cloning of BsrGI-BamHI fragment into PDE8A_c8_2010; ***E***-Hypothetical result of the next step - incorporation of BsrGI-BsrGI fragment into PDE8A_oprI8_R14

4.1.3 2nd mutagenesis

Primer 8a_opr_II was designed to repair point mutation at A806G and covered also NsiI restriction site at nt 835. Then in combination with 8a_opr_I it was used to perform 2nd mutagenic PCR (for details see methods). Amplified segment was cloned into p-GEM T-easy vector system and transferred into bacteria. Isolated strain produced PDE8a_H2 plasmid that proved to be without amino acid changing mutation in PDE8a gene.

Segment between SacII and BsrGI from PDE8a_opr-I8_R14 (nt 135-323) was transferred into PDE8a_H2, yielding construct PDE8a_H2Rb-pGEM. Primer 8a_opr_II include Nsi restriction site that in concert with NsiI site found in multiple cloning site of pGem allowed the transfer of nt (835-2487) from PDE8a_oprI8-pGEM into cloned into PDE8a_H2Rb-pGEM resulting in construct PDE8a_H2Rb1.

Prepared construct PDE8a_H2Rb1 contained PDE8A1 coding sequence from 2nd SacII restriction site (at 135th nt) till the end of the coding sequence and was important intermediate for generation of N-terminal variants as well as for catalytically inactivated PDE8A1.

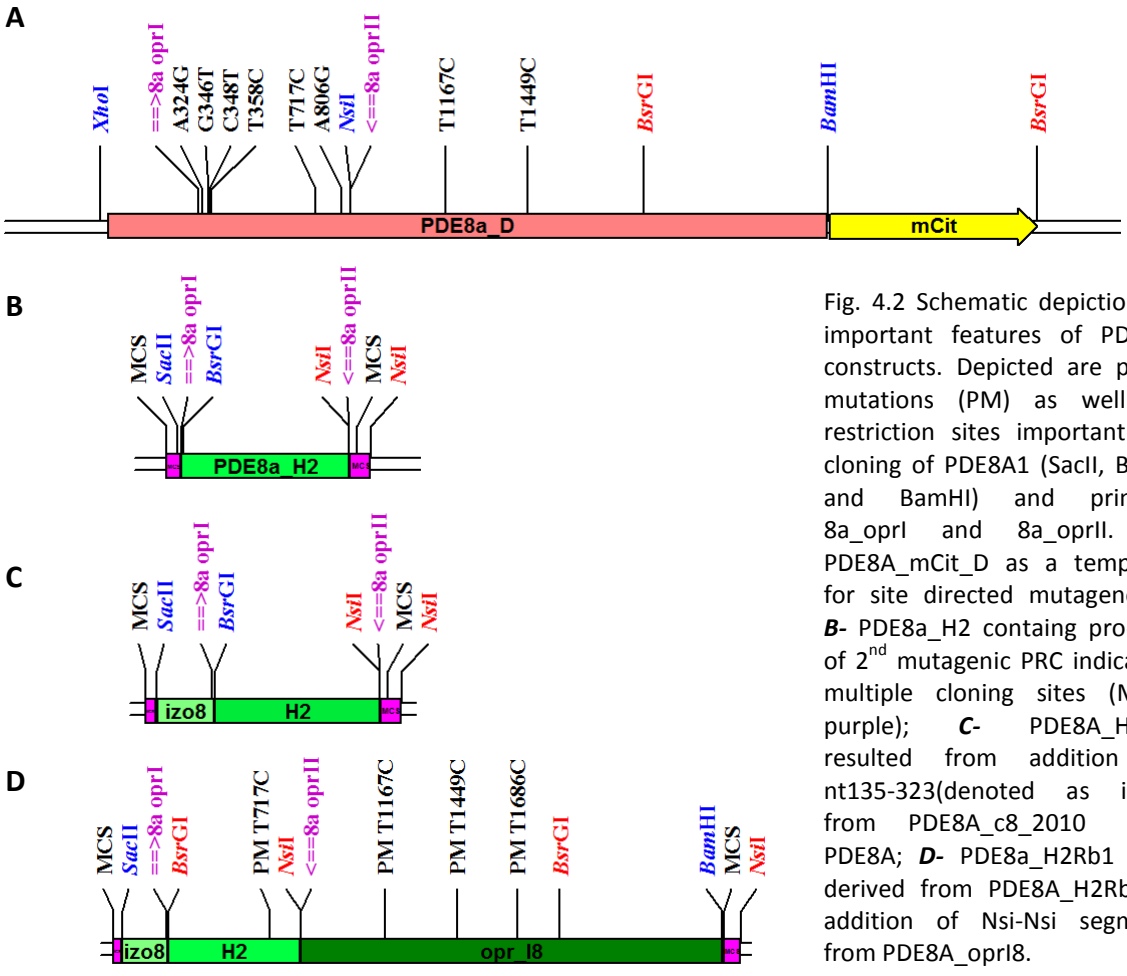

Fig. 4.2 Schematic depiction of important features of PDE8A constructs. Depicted are point mutations (PM) as well as restriction sites important for cloning of PDE8A1 (SacII, BsrGI and BamHI) and primers 8a_oprI and 8a_oprII. ***A***- PDE8A_mCit_D as a template for site directed mutagenesis; ***B***- PDE8a_H2 containg product of 2nd mutagenic PRC indicated multiple cloning sites (MCS; purple); ***C***- PDE8A_H2Rb resulted from addition of nt135-323(denoted as izo8) from PDE8A_c8_2010 to PDE8A; ***D***- PDE8a_H2Rb1 was derived from PDE8A_H2Rb by addition of Nsi-Nsi segment from PDE8A_oprI8.

4.1.4 Construction of N-terminal variants

After construction of PDE8a_H2Rb1 the next step was to transfer the whole repaired construction from pGEM into mCit plasmid background. This was done by cloning segment between SacII and BamHI (nt 135-2487) from PDE8a_H2Rb1 into PDE8A(N-WT)-mCit which contained PDE8a coding sequence from start codon to the second SacII restriction site (nt 1-135). However SacII was cutting the DNA in two places (at nt 63 and 135) close by each other and the piece between the two restriction sites was lost during cloning. Once the big construct from H2Rb1 was safely in mCit vector (plasmid PDE8a_H2Rb16R) the short piece from in between SacII restriction sites (nt 64-135) was put back by another cloning step resulting in the PDE8a_H2Rb16Rb. In PDE8a_H2Rb16Rb the whole coding sequence of PDE8A1 was assembled a further on the construct was named PDE8A(WT)-mCit (Fig. 4.3).

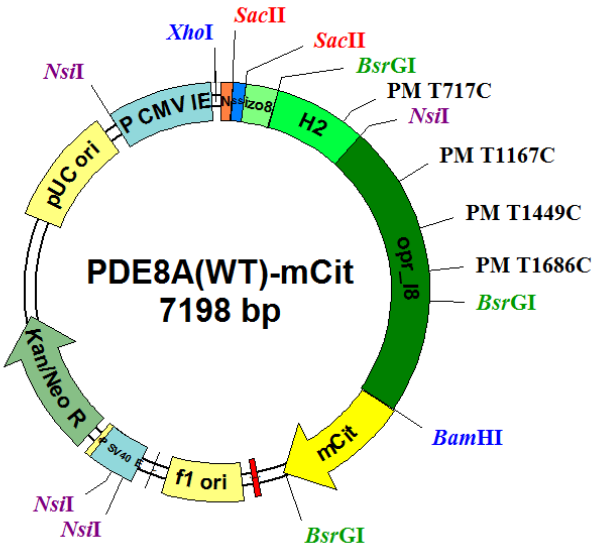

Fig. 4.4 Construct PDE8A(WT)-mCit. Depicted are point mutations (PM), sites recognized by restriction enzymes and origins of particular segments. N-segment coding for N-terminal fragment of PDE8A1 protein (orange) comes from PDE8A(N-WT)-mCit; SS-segment (blue) is localized between the two SacII restriction sites, segment was lost during transfer of PDE8A1 (nt 135-2487) into PDE8A(N-WT)-mCit and was added back; izo_8 segment (pale green) comes from PDE8A_c8_2010; H2 segment (bright green) is the cloned product of 2nd mutagenic PCR and opr_I8 segment (dark green) comes from PDE8A_oprI8-pGem; The remaining features depicted on the plasmids feature of the vector. For details see chapter "vectors".

Since constructs coding for N-terminal segments of PDE8A with altered acylation pattern were already prepared in previous work (tab. 4.3), to construct full-length PDE8A localization variants it was needed to transfer each of thethis constructs (nt 1-64) into PDE8A(WT)-mCit. This procedure included cloning of the corresponding segments into PDE8A(WT)-mCit via XhoI and SacII restriction enzymes. Segment between the SacII sites

(nt 64-135) was lost during the cloning and was put back subsequently by another cloning step.

construct designation	postranslational modification	mutation in protein sequence
PDE8A(N-WT)-mCit	N-myristoylation; palmytoylation	-
PDE8A(N-M)-mCit	N-myristoylation	C3S
PDE8A(N-P)-mCit	palmytoylation	G2A
PDE8A(N-0)-mCit	none	G2A, C3S

Tab. 4.3 List of constructs coding for N-terminal fragment of PDE8A1 with putative posttranslational modification. Mutation that cause the altered acylation of PDE8A1 N-terminal fragments are listed on the right

.

By assembling of PDE8A1(WT)-mCit and its acylation variants first phase of this diploma thesis was finished successfully and first of the goals was achieved.

4.1.5 Preparation of catalytically inactivated PDE8a

Cells expressing PDE8a-mCit, were often observed as losing adherence and never survived in culture for longer time – over two days. In case of Raw264 cells, there were hardly any PDE8a expressing cells observed after less than 24 hours. When compared the transfection efficiency of PDE8a-mCit was twice as low as that of its corresponding PDE8a_N-mCit constructs and the expression level differed in orders of magnitude as was obvious from data obtained from flow cytometry.

The observed phenomenon raised the question whether this was due to the size difference between transfected constructs, or due to the cAMP hydrolyzing activity of PDE8a. In order to determine the cause of it, we have decided to produce catalytically inactivated PDE8a. Construction of catalytically inactivated PDE4d5s and 3D has been published previously and was based on mutation of Asp^{556} to alanine at that position (Perry et al 2002). Based on sequence alignment PDE8A and PDE4D residue corresponding to Asp^{556} in PDE4D was identified as Asp^{726} in PDE8A. Comparison of 3D structures of PDE4D and PDE8A available in the MMDB database, further confirmed that Asp^{726} of PDE8A is in position crucial for catalysis and is part of metal binding pocket (Fig. 4.4).

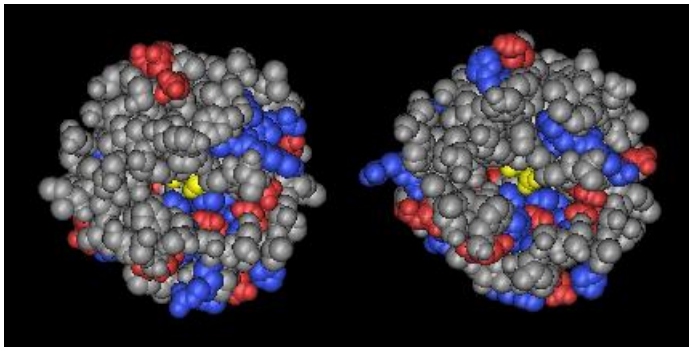

Fig. 4.4 The 3D structures of catalytic domain PDE8A (on the left; MMDB id 68150) and PDE4D (right; MMDB id 94628). Asp 726 of PDE8A and Asp 556 of PDE4D are colored yellow and within the catalytic pocket occupy the same position. Structures were visualized by CN3D software (NCBI), displayed are residues within the range 14 angstroms from the marked aspartate

Construct coding for catalytically inactivated PDE8A1 has been prepared by site directed mutagenesis (see methods) and determination of the coding sequence confirmed that produced protein should indeed be inactive. However it biological activity was not yet examined.

4.1.6 Construction of PDE8A(N-WT)-mStraw

In order to compare localization of full-length PDE8A1 with its N-terminal fragment, the citrine coding region in construct PDE8A(N-WT)-mCit was replaced by sequence coding for strawberry fluorescent protein yielding construct PDE8A(N-WT)-mStraw. This construct was crucial for simultaneous observation of expressed N-terminal fragment as well as full-length PDE8A1 that might provide information about factors that determine distribution of PDE8A1 in living cells.

4.2 Localization of PDE8A1 in relation to acylation of its N-terminus

4.2.1 Raw264.7

To examine localization pattern of different acylation variants of PDE8a prepared DNA constructs were transfected into RAW264.7 cells and their localization in relation to cellular structures was determined (Fig 4.5) and summarized in tab 4.4.

construct designation	postranslational modification	Localization
PDE8A(WT)-mCit	N-myristoylation; palmytoylation	plasmatic membrane
PDE8A(N-WT)-mCit	N-myristoylation; palmytoylation	plasmatic membrane, vesicles
PDE8A(M)-mCit	N-myristoylation	perinuclear membranes
PDE8A(N-M)-mCit	N-myristoylation	perinuclear membranes, cytosol
PDE8A(P)-mCit	palmytoylation	cytosolic
PDE8A(N-P)-mCit	palmytoylation	cytosolic
PDE8A(0)-mCit	none	cytosolic
PDE8A(0)-mCit	none	cytosolic

Tab 4.4 Summary of localization of PDE8A constructs in Raw264.7 cells

Fig. 4.5 Localization of PDE8A constructs in Raw264.7 cells (on the next page) Raw cells were transfected with PDE8A(WT)-mCit PDE8A(N-WT)-mCit PDE8A(M)-mCit PDE8A(N-M)-mCit PDE8A(P)-mCit PDE8A(N-P)-mCit PDE8A(0)-mCit PDE8A(0)-mCit. Cells were stained with mitotracker red; transferin -AF594 and Phalloidin-AF594 as described in methods. Imagined by Olympus XI-81 Cell'R'microscopic sytem; 60x objective with immersion oil.

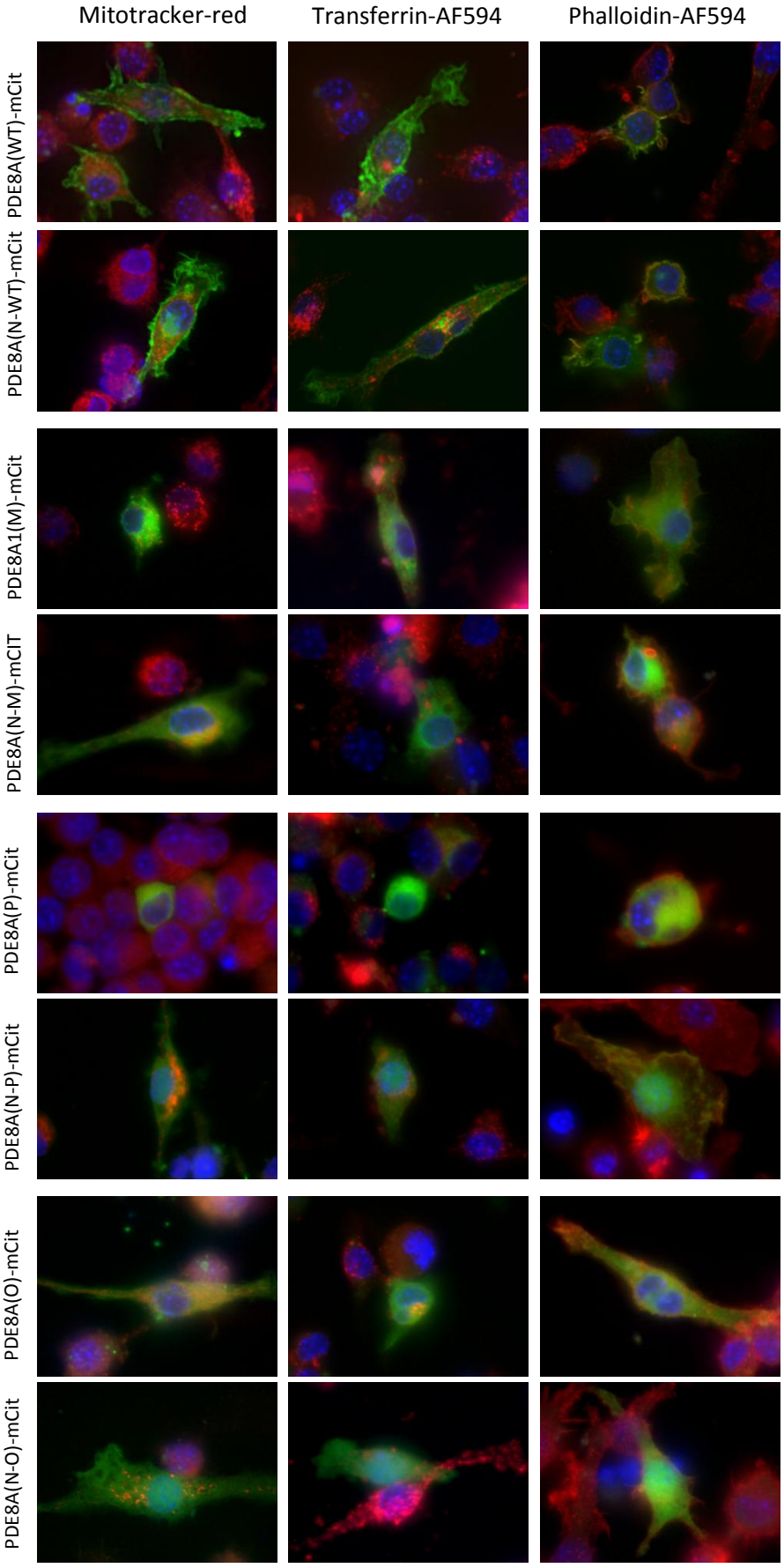
Mitotracker-red
Transferrin-AF594
Phalloidin-AF594
PDE8A(WT)-mCit
PDE8A(N-WT)-mCit
PDE8A1(M)-mCit
PDE8A(N-M)-mCIT
PDE8A(P)-mCit
PDE8A(N-P)-mCit
PDE8A(O)-mCit
PDE8A(N-O)-mCit

4.2.2 CHO cd11

Distribution of full-length PDE8A constructs within CHO cd11 cells was examined. The results correspond well with the distribution in Raw264.7 cells. However in CHO cd11 perinuclear localization of PDE8A1(M)-mCit is more pronounced (Fig. 4.6).

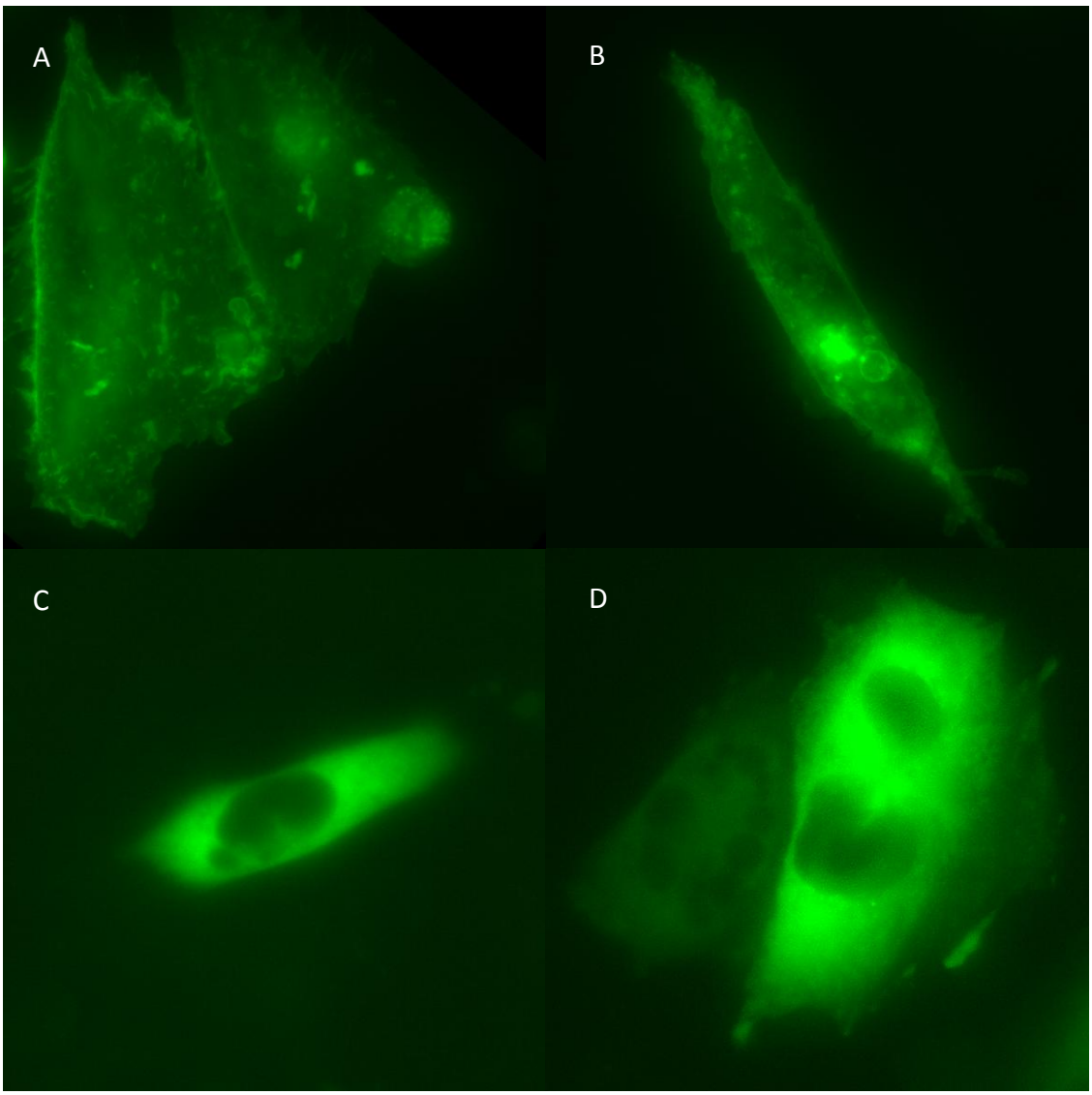

Fig. 4.6 CHO cd11 cells transfected with: ***A-***PDE8A(WT)-mCit; ***B-*** PDE8A(M)-mCit; ***C-*** PDE8A(P)-mCit ***D-*** PDE8A(0)-mCit; Olympus XI-81 Cell'R' microscopic system 60X objective

4.2.3 Contransfection of PDE8A(N-WT)-mStraw with PDE8A(WT)-mCit and confocal microscopy in living cells

To examine whether there are additional factors that determine subcellular localization of PDE8A1 apart from the its acylation at the N-terminus, CHO cd11 cells were transfected by a approximately equimolar mixture of PDE8A(N-WT)-mStraw with PDE8A(WT)-mCit and observed by confocal microscope.

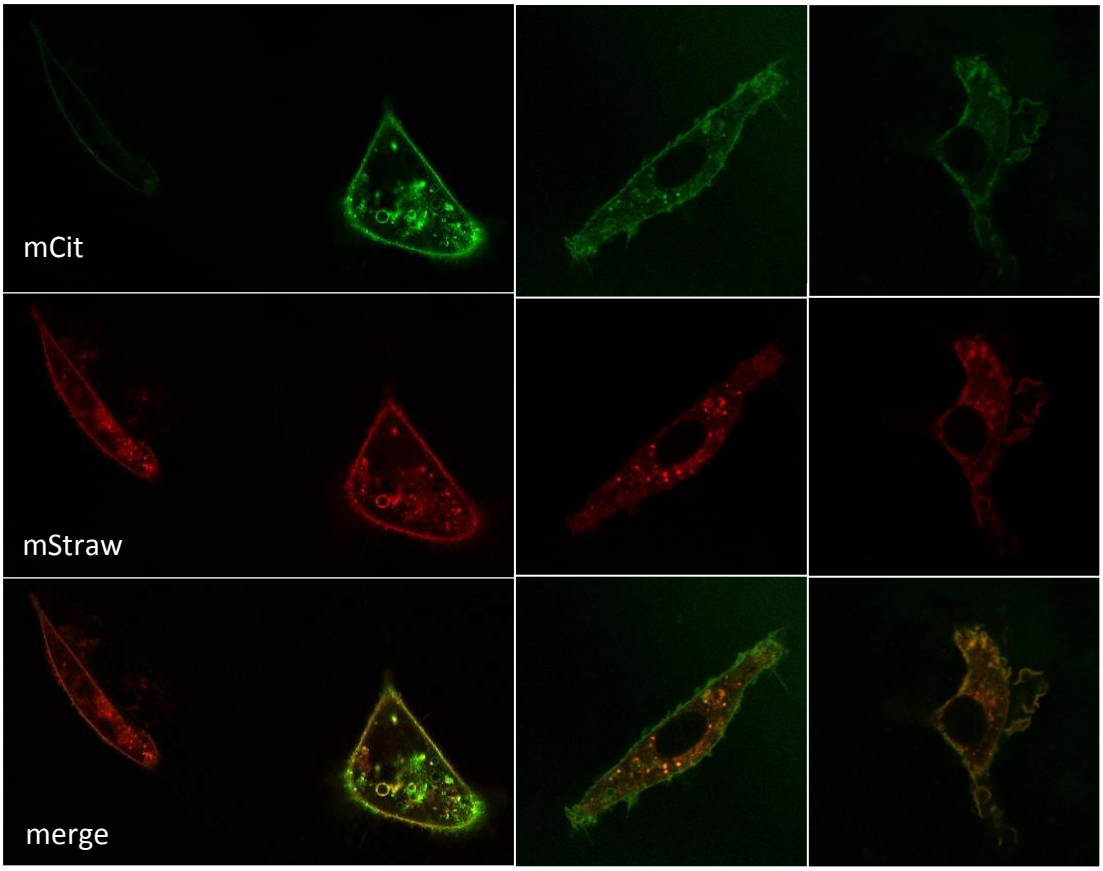

Fig. 4.6 CHO cd11 cells transfected with both PDE8A(WT)-mCit and PDE8A(WT)-mStraw; On the very left cell transfected only by mStraw is depicted, the rest of the cells are expressing both fluorescent tags. Cell were imaged as described in 3.2.10

4.3 PDE8A1 vs CyaA: Examining the rivalry in living cells

4.3.1 Toxic effect of PDE8A1-mCit

During microscopic studies we have noted that cells expressing full-length catalytically active PDE8a vanished quickly from the culture. We have concluded that presence of high amount of PDE8a is toxic to cells expressing it and confirmed this first with RAW264.7 cells (obviously the most sensitive cell line from tested). Major decrease of cells expressing full/length PDE8a in proportion to non-transfected ones was observed between 12th and 24th hours after transfection. This toxic effect was abolished in truncated N-terminal variants (Fig. 4.7).

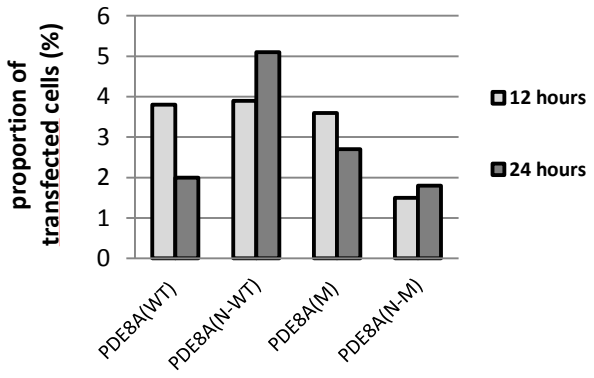

Fig. 4.8s Proportion of RAW 264.7 expressing mCit as a result of transfection by: PDE8A(WT)-mCit, PDE8A(N-WT)-mCit, PDE8A(M)-mCit, PDE8A(N-M)-mCit after 12 and 24 hours. Note the decrease of cells expressing full-length PDE8A-mCit and increase of cells expressing PDE8A N-terminal constructs. Data shown comes from single preliminary experiment. All cell counts were determined by BD-LSRII and using BD FACSDiva software;

In the other cell line tested, CHO cd11, the majority cells expressing PDE8a1 was floating in the medium already 16 hours after transfection. Under optimal conditions CHO cd11 cells are adherent, thus their inability to adhere can be considered a sign of the altered physiological state (fig 4.9 on the next page).

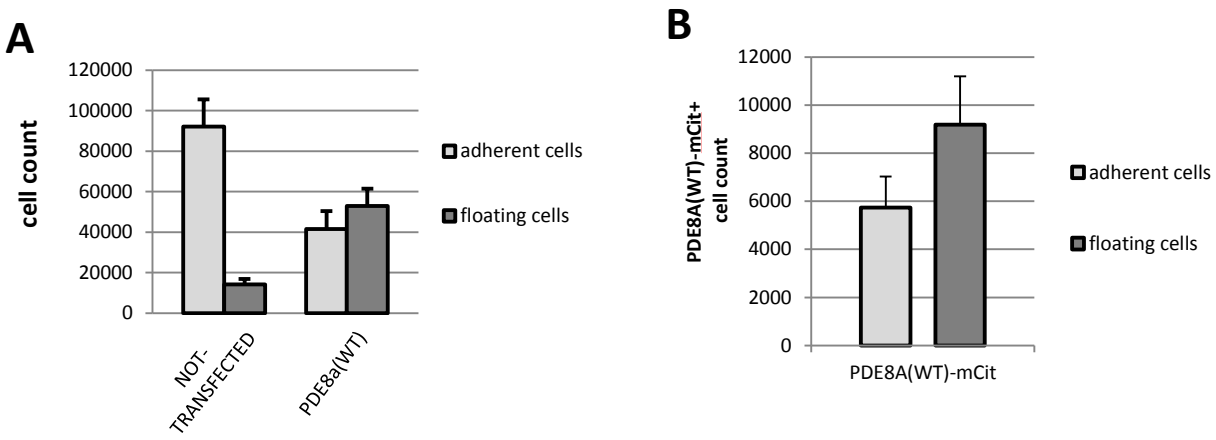

Fig 4.9 A- Cells not transfected or transfected by PDE8A(WT)-mCit as found in either supernatant (floating) or on cultivation surface (adherent); B- Count of CHO cd 11 cells expresing PDE8A(WT)-mCit adherent or floating; A,B cell counts were evaluated 16 hours after transfection; harvested cells were centrifuged and resupsended in the same volume of PBS so that the counts from supernatant and cultivation would be proportional; data shown comes from three parallel experiments; Error bars indicate the standard deviation. All cell counts were determined by BD-LSRII and using BD FACSDiva software;

We have decided to investigate this phenomenon in better detail and challenge the PDE8A1 expressing cells with cyclase toxin of *Bordetella pertussis*. The reasoning behind the involvement of the CyA toxin into the experimental setup is as follows:

4.3.2 The design of the experimental system

Bordetella pertussis is known to express several bioactive proteins including toxin with adenylyl cyclase activity that translocate it´s cyclase domain into cytosol of target cells and accumulate in lipid rafts (Bumba et al 2010). PDE8a was predicted to be part of membrane RAFT-like microdomains due to its N-terminal double-acylation (Falteisek 2008).

We decided to test the hypothesis. For this design of the procedure, protein-protein targeting interaction of PDE8a and other proteins have been considered negligible in cells expressing PDE8A as result of transfection. Protein-protein targeting interactions of Cya A have been also considered of less importance. Based solely on shared preferences for lipid environment PDE8A and CyA should be colocalized in similar/identical type of membrane microdomains and therefore functionally interfere. If such a co-localization really occurs there should potentially be a concentration of PDE8a and cyaA high enough enabling two enzymes to compensate for their catalytic and thus toxic resulting in lowered toxicity for both of the “rivaling” enzymes in the cell. Cell in which the “balance

of enzymatic power" will be achieved should be more viable, since cells that do not express any PDE8A should be intoxicated by Cya A and those expressing too much PDE8A will die in result of PDE8A expression

Since the beginning we were aware, that all these assumptions may be incorrect. However we were still interested in what would happen, shall the concerned enzymes meet (face to face) in one cell.

Originally we intended to FACSort out PDE8A1-mCit expressing cells and measure cAMP concentration in cells after challenge of cya A. Measuring concentration in this way would require excessive amount of cells for analysis, however due to low transfection efficiencies of full length PDE8a constructs in relevant cell types (RAW, CHO CD11) this would subsequently require enormous cultivation surfaces and amounts of DNA, so this alternative was not considered as favorable. Moreover, interpretation of measured cAMP concentration would be very complicated, since it will not directly refer to the cell viability or physiological status in context of PDE8A. Due to this reasons we have banned this experimental procedure.

As was already mentioned above, we decided to test the hypothesis, whether the balance of power between PDE8A and Cya A could be achieved and is of physiological relevance in transfected cells with the outcome - beneficial effect on viability of PDE8A expressing cells (in the context of Cya A and vice versa). We have finally decided to challenge PDE8a-mCit expressing cell with CyA in mixed culture of transfected and non-transfected cell and analyze the complex cell suspension using FACS analysis. Measuring the mixed culture would provide information about viability of PDE8A-mCit expressing cells in relation to the viability of non-transfected ones in the complex system with the toxin involved. Important advantage of this setup is that the fluorescence signal in the transfected cell is proportional to the amount of PDE8A itself – and could be quantitatively correlated to the potential functional effect on the cell survival using particular concentration of the Cya A toxin.

4.3.3 Proportion of PDE8A1(WT)-mCit but not PDE8A1(N-WT) expressing cells is increased after challenge by cya A

CHO cd11 cells transfected by either PDE8A1(WT)-mCit or PDE8A1(N-WT)-mCit have been challenged by different concentration of cya A 12 hours after transfection.

Examined were 3 different concentrations of 1, 5 and 45 ng of toxin in 500µl of medium per 1/24-well plate corresponding to 1.9 cm^2 cultivation surface. Then, 20 hours after addition of toxin. Proportion of cells expressing the fluorescent tag within the surviving population was evaluated by flow cytometry (Fig. 4.10). Challenge of sample by cya A caused enrichment of PDE8A1(WT)-mCit expressing cells in the population of living cells. In cells, not treated with cya A, 15.6% of cell expressed PDE8A1(WT)-mCit, while this proportion has risen to 22.9, 21.6 and 22.0 when 1, 5 or 45 ng of cya A were used respectively. In contrast proportion of PDE8A1(N-WT)-mCit was decreasing in response to increasing concentrations of cya A.

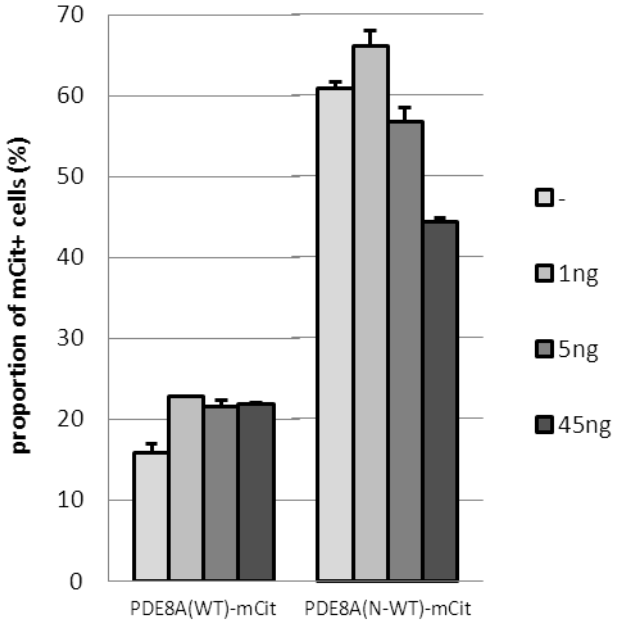

FIG.X Proportion of cells expressing PDE8A1(WT)-mCit; PDE8A1(N-WT)-mCit within the population of living cells. Determined by flow cytometry where cells not stained by EtBr and with FSC-A values similar to those of control healthy cells were considered alive. Total amounts of cya A added to wells indicated in the legend Data shown are mean of two parallel experiments. Error bars indicate standard deviation

4.3.4 Acylation pattern of PDE8A1 determines its interplay with cya A

Preliminary data collected showed that expression of PDE8A1(WT) may have some protecting effect, in case of Cya A challenge. It has been verified that modified acylation pattern of PDE8A1 variant directed produced proteins into different cellular compartments (chapter xxx). Cellular localization pattern of PDE8A1 could therefore play crucial role upon treatment by Cya A. To test whether localization of PDE8A1 matters in Cya A intoxication, CHO cd 11 cells were transfected with the PDE8A1-mCit constructs

encoding variants with the different acylation motif (double-acylated, myritoylated only, palmitoylated only, without acylation) . Twenty hours after transfection cells were challenged by incubation with 200ng Cya A in 200µl of DMEM medium for 3 hours and analyzed subsequently.

For determination of cell viability we used in parralel combination of DAPI and FSC and staining by annexin V combined with FSC.

Quantitation of the toxicity (using DAPI) yielded the following results:

When untreated, 11.2% of living cells expressed PDE8A1(WT)-mCit, however after treatment by cya A it was 18.6% of the living cells that expressed PDE8A1(WT)-mCit. Similarly, 12.3 % of living cells expressed PDE8A1(M)-mCit, but after treatment by Cya A this number has reached 18.6%. Proportion of cells expressing PDE8A1(P)-mCit or PDE8A1(O)-mCit was not increased after Cya A challenge.

Staining by annexin V distinguishes apoptotic from non-apoptotic cell. In the population of non-apoptotic cells, increase from 15.8% to 18.0% of PDE8A1(WT)-mCit was observed after treatment with Cya A. Again (similarly to PDE8A1(WT)-mCit) increase from 15.7% to 20.4% in the case of myristoylated form PDE8A1(M)-mCit was observed. Proportion of other two variants has decreased upon challenge by Cya A – indicating the lack of the Cya A mediated protection and induction of the Cya A mediated cytotoxicity.

In summary, proportion of PDE8A1 expressing cells has been increased upon Cya A challenge in the case of PDE8A1(WT)-mCti and PDE8A1(M)-mCit (both exhibiting membrane localization) however remained constant (or decreased) in the case of other two PDE8A1 variants that exhibit homogenous distribution across the cytosol.

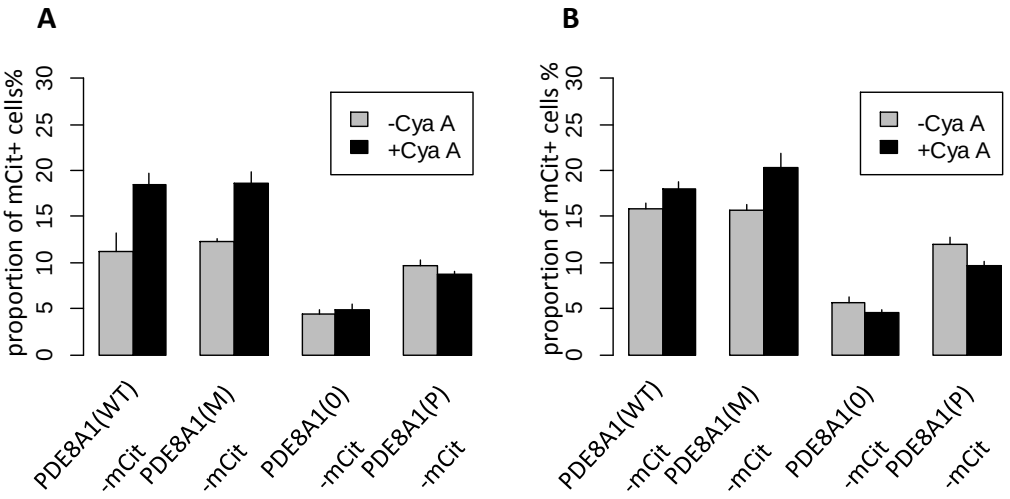

Fig.4.11: Proportion of PDE8A1-mCit expressing cells (acylation variant indicated at X-axis) in population of living cells as determined by flow cytometry. Left (A) living cells were determined by FSC and dapi staining; Right (B) Non-apoptotic cells as determined by Annexin V staining. Error bars indicate standard deviation. Values shown are mean from three parallel experiments.

5 Discussion

5.1 Alternative splicing and construction of PDE8A1-mCit variants

In thesis presented here, preparation of fluorescently labeled PDE8A1 constructs with altered acylation variant is reported. Several problems were encountered during construction of full-length PDE8A1-mCit encoding plasmid.

First it was impossible to amplify 5' terminal region of the coding sequence from cDNA libraries by PCR experienced within the frame of previous work with PDE8A1 conducted in our laboratory (Falteisek 2008). A similar problem occurred during the first cloning and characterization of human PDE8A, where authors state that, despite their extensive effort they were not capable of PCR amplification of longer PDE8A sequence than they actually report although they predict its existence (Fisher et al 1998). Detailed examination of PDE8A gene organization revealed high CG content around the 5' terminal region of the ORF that might be the cause resistance of this region to PCR amplification (Wang et al 2001, Glavas et al 2001).

Second problem restraining the cloning of PDE8A1 was alternative splicing. There were several clones of PDE8A with different exon composition. Alternative splicing is a common trait among PDE genes (see chapter X.Y, Conti and Beavo 2007) and it has already been reported (Wang et al 2001). However there are very few studies that would focus on addressing the alternative splicing of PDE8A. The one available is concerned with PDE8A transcripts found only in testis and $CD4^+$ lymphocytes, yet there are more tissues, where PDE8A transcripts are present, such as spleen or colon (Wang et al 2001). Thus alternative splicing of PDE8A has not been assessed in detail so far. In this study new splice variants and putative novel exons are reported. The exon/intron boundaries correspond well with those already known and the novel putative exons reported are found within the region of PDE8A gene. Sequences neighboring the novel segments in the clones are found separated from them in genome sequence, thus suggesting that they are exons indeed.

The last problem was that all the clones generated at the beginning of PDE8A project (during several rounds of preparation) differed in DNA sequence from sequence reported as canonical (GI:47132535) altering amino acid sequence in translated protein. After Although the resulting amino acid substitutions are not localized in regions with reported

function (uniprot entry O60658 - PDE8A_HUMAN), we considered to be on a safe side avoiding unpredictable consequence that might be hard to recognize retrospectively. Thus we decided to eliminate mutations.

Considering the available collection of clones and the troubles that *de novo* cloning of PDE8A has brought to others, it seemed that combining and repairing the available clones may be easier way to obtain PDE8A1 canonical coding sequence. Although additional point mutations to be corrected were generated and discovered during the procedure, finally time-consuming effort lead to the desired goal and PDE8A1 tagged with citrine on its C-terminus was obtained.

5.2 Catalytically inactive PDE8A1

For further experiments with PDE8A1 in mammalian cells its catalytically inactive variant represents an important control. Although biological activity of protein encoded by the prepared construct has not been assessed, recently another unrelated group prepared D726A PDE8A1 and considered it catalytically dead (Brown et al 2012). Although, no direct proof has been published yet and only indirect indications are available, it is most probable that D726A PDE8A1 lacks cAMP hydrolyzing activity. Most likely, although independent, both preparations of catalytically inactive PDE8A1 use the same substantiation.

5.3 Localization of PDE8A1

Localization of PDE8A1 was examined in Raw264.7 and to lesser extent also in CHO cells. Observation confirmed previous notion of Lukáš Falteisek that distribution of PDE8A1 is determined by both N-myristoylation (Gly^2) and palmitoylation of Cys^3 (Falteisek 2008). Although posttranslational modification such as phosphorylation sites, N-myristoylation and amidation have been predicted for PDE8A (Wang et al 2001, Gamanuma et al 2003) none of them has been experimentally confirmed until recently (Brown et al 2012). The only known posttranslational modification is phosphorylation of by PKA at serine 359 that activates the PDE8A catalytic activity (Brown et al 2012).

Moreover parallel observation of PDE8A(N-WT)-mStraw with PDE8A(WT)-mCit suggested slightly different localization of N-terminal fragment in comparison to full-length constructs. This indicates that some other factor, such as interaction domain PAS

identified in PDE8A1 (Soderling et al 1998, Wang et al 2001, Wu et al 2004), may play important role in directing localization of PDE8A.

Here provided evidence for the first time demonstrates that both N-myristoylation as well as N-palmytoylation alters the distribution of full length PDE8A1 within the cell.

5.4 PDE8A1 and cya A

Experimental system to address biological interaction of PDE8A1 and cya A was designed. It should be noted that environment in which the interaction was tested is rather artificial for both proteins. First of all expression levels of PDE8A1 are unusually high in this system. Moreover CHO cells are adherent cell line with epithelial morphology derived from Chinese hamster ovaries, while target cells for cya A are mostly phagocytic cells of immune system. On the other in this way not the fine tuning but the robustness of the cAMP system is addressed.

Observed was modest increase in viability of PDE8A(WT)-mCit and PDE8A(M)-mCit transfectants upon challenge by cya A. Both of the produced proteins shared membrane localization although PDE8A(M)-mCit preferred endomembrane structures, most probably endoplasmatic reticulum (Falteisek 2008) over the cytoplasmic membrane and PDE8A(WT)-mCit was found almost exclusively on cytoplasmic membrane. There was basically no difference in viability of other two constructs whether the toxin was added or not.

There are several possible reasons for this observation. First is the activity of proteins with different localization that might be different and differently regulated. Activity of PDE8A1 is increased by interaction with β-arrestin or PKA (Wu et al 2004, Brown et al 2012) this activation might not be possible for soluble mutant protein. Moreover N-terminal fragment of PDE8A1 is important for the regulation of its activity (Wang et al 2008) and non-acylated N-terminus may prefer conformation not suitable for catalytic activity. Moreover the soluble variants may be undergoing degradation or be otherwise restricted in activity. Other possible explanation is that cytosolic PDE8A1 mutants are fully active and it is indeed due to the different localization

Provided data are considered preliminary and before driving definitive conclusions additional properties of PDE8A1 have to be evaluated otherwise the interpretation of this data may lead into speculation very easily.

6 Conclusions

Construction of PDE8A1

- Fluorescently tagged full length PDE8A1 was successfully constructed (PDE8A1(WT)-mCit)
- Three localization variants of PDE8A1 were prepared, namely:
  - PDE8A(M)-mCit (coding for N-myristoylated protein)
  - PDE8A(P)-mCit (coding for palmytoylation at Cys^3)
  - PDE8A(0)-mCit (coding for non-acylated protein)
- Construct coding for catalytically inactivated PDE8A1 was prepared
- Construct PDE8A(N-WT)-mStraw coding for N-terminal fragment of PDE8A1 tagged with mStrawberry fluorescent protein suitable for study of colocalization of full-length PDE8A1 and its N-terminal fragment

Localization of PDE8A1

- Double acylated full length PDE8A1 (PDE8A(M)-mCit) was found to localize to cytoplasmic membrane of both Raw264.7 and CHO cd11 cells
- Myristoylated full length PDE8A1 (PDE8A(M)-mCit) was found to localize to perinuclear membran of both Raw264.7 and CHO cd11 cells. Additionally it was found to diffuse freely in the cytosol of Raw264.7
- Mutant proteins that lacked myristoylation (PDE8A(P)-mCit and PDE8A(0)-mCit) diffused freely in the cytoplasm
- Full length PDE8A1 with double acylation exhibited slightly different distribution than the corresponding N-fragment

Cytotoxicity of PDE8A1 and Cya A

- Expression of full length PDE8A1 (duble acylated –WT and myristoylated – M) was found toxic, while expression of corresponding N fragments was not
- Full-length PDE8A1 with membrane localization (duble acylated –WT and myristoylated – M) provided modest protection from intoxication by Cya A for cells expressing them, while PDE8A1 variants with cytoplasmic localization did not

7 References

1. Aronoff, D.M., Canetti, C., Serezani, C.H., Luo, M. & Peters-Golden, M. Cutting edge: macrophage inhibition by cyclic AMP (cAMP): differential roles of protein kinase A and exchange protein directly activated by cAMP-1. *J Immunol* **174**, 595-599 (2005).
2. Aronoff, D.M., Carstens, J.K., Chen, G.H., Toews, G.B. & Peters-Golden, M. Short communication: differences between macrophages and dendritic cells in the cyclic AMP-dependent regulation of lipopolysaccharide-induced cytokine and chemokine synthesis. *J Interferon Cytokine Res* **26**, 827-833 (2006).
3. Bader, S., Kortholt, A. & Van Haastert, P.J. Seven Dictyostelium discoideum phosphodiesterases degrade three pools of cAMP and cGMP. *Biochem J* **402**, 153-161 (2007).
4. Baillie, G.S. *et al.* TAPAS-1, a novel microdomain within the unique N-terminal region of the PDE4A1 cAMP-specific phosphodiesterase that allows rapid, Ca2+-triggered membrane association with selectivity for interaction with phosphatidic acid. *J Biol Chem* **277**, 28298-28309 (2002).
5. Ballinger, M.N., Welliver, T., Straight, S., Peters-Golden, M. & Swanson, J.A. Transient increase in cyclic AMP localized to macrophage phagosomes. *PLoS One* **5**, e13962 (2010).
6. Beavo, J.A. & Brunton, L.L. Cyclic nucleotide research -- still expanding after half a century. *Nat Rev Mol Cell Biol* **3**, 710-718 (2002).
7. Beca, S., Aschars-Sobbi, R., Panama, B.K. & Backx, P.H. Regulation of murine cardiac function by phosphodiesterases type 3 and 4. *Curr Opin Pharmacol* **11**, 714-719 (2011).
8. Bodor, J. *et al.* Cyclic AMP underpins suppression by regulatory T cells. *Eur J Immunol* **42**, 1375-1384 (2012).
9. Bolger, G.B. *et al.* Scanning peptide array analyses identify overlapping binding sites for the signalling scaffold proteins, beta-arrestin and RACK1, in cAMP-specific phosphodiesterase PDE4D5. *Biochem J* **398**, 23-36 (2006).
10. Brown, K.M., Lee, L.C.Y., Findlay, J.E., Day, J.P., Bailie, G.S. Cyclic AMP-specific phosphodiesterase, PDE8A1, is activated by protein kinase A-mediated phosphorylation. FEBS Letters 586, 1631–1637 (2012).
11. Bumba, L., Masin, J., Fiser, R., Sebo, P. Bordetella Adenylate Cyclase Toxin Mobilizes Its beta(2) Integrin Receptor into Lipid Rafts to Accomplish Translocation across Target Cell Membrane in Two Steps. PLOS Pathogens 6 (2010).
12. Cebecauer, M., Owen, D.M., Markiewicz, A. & Magee, A.I. Lipid order and molecular assemblies in the plasma membrane of eukaryotic cells. *Biochem Soc Trans* **37**, 1056-1060 (2009).
13. Charych, E.I., Jiang, L.X., Lo, F., Sullivan, K. & Brandon, N.J. Interplay of palmitoylation and phosphorylation in the trafficking and localization of phosphodiesterase 10A: implications for the treatment of schizophrenia. *J Neurosci* **30**, 9027-9037 (2010).
14. Conti, M. & Beavo, J. Biochemistry and physiology of cyclic nucleotide phosphodiesterases: essential components in cyclic nucleotide signaling. *Annu Rev Biochem* **76**, 481-511 (2007).
15. Cooper, D.M.F. Regulation and organization of adenylyl cyclases and cAMP. Biochem. J. 375, 517-529 (2003).
16. Cotton, M., Claig, A. G protein-coupled receptors stimulation and the control of

cell migration. Cellular signaling 21, 10465-1053 (2009).
17. Cukkemane, A., Seifert, R. & Kaupp, U.B. Cooperative and uncooperative cyclic-nucleotide-gated ion channels. *Trends Biochem Sci* **36**, 55-64 (2011).
18. de Rooij, J. *et al.* Epac is a Rap1 guanine-nucleotide-exchange factor directly activated by cyclic AMP. *Nature* **396**, 474-477 (1998).
19. Delint-Ramirez, I., Willoughby, D., Hammond, G.V., Ayling, L.J. & Cooper, D.M. Palmitoylation targets AKAP79 protein to lipid rafts and promotes its regulation of calcium-sensitive adenylyl cyclase type 8. *J Biol Chem* **286**, 32962-32975 (2011).
20. Dodge, K.L. *et al.* mAKAP assembles a protein kinase A/PDE4 phosphodiesterase cAMP signaling module. *EMBO J* **20**, 1921-1930 (2001).
21. Dodge-Kafka, K.L. *et al.* The protein kinase A anchoring protein mAKAP coordinates two integrated cAMP effector pathways. *Nature* **437**, 574-578 (2005).
23. Dong, H., Osmanova, V., Epstein, P.M. & Brocke, S. Phosphodiesterase 8 (PDE8) regulates chemotaxis of activated lymphocytes. *Biochem Biophys Res Commun* **345**, 713-719 (2006).
24. Douglass, A.D. & Vale, R.D. Single-molecule microscopy reveals plasma membrane microdomains created by protein-protein networks that exclude or trap signaling molecules in T cells. *Cell* **121**, 937-950 (2005).
25. Edwards, H.V., Christian, F. & Baillie, G.S. cAMP: novel concepts in compartmentalised signalling. *Semin Cell Dev Biol* **23**, 181-190 (2012).
26. Falteisek, L. Cloning and characterization of proteins potentialy targeted to the membrane microdomains. Diploma thesis. 99 pp., Prague 2008.
27. Fisher, D.A., Smith, J.F., Pillar, J.S., Denis, S.H., Cheng, J.B. Isolation and charakterisation of PDE8A, a novel human cAMP-specific phosphodiesterase. BBRC 246, 570-577 (1998).
28. Francis, S.H., Colbran, J.L., McAllister-Lucas, L.M. & Corbin, J.D. Zinc interactions and conserved motifs of the cGMP-binding cGMP-specific phosphodiesterase suggest that it is a zinc hydrolase. *J Biol Chem* **269**, 22477-22480 (1994).
29. Gamanuma, M., Yuasa, K., Sasaki, T., Sakurai, N., Kotera, J., Omori, K. Comparison of enzymatic characterization and gene organization of cyclic nucleotide phosphodiesterase8 family in humans. Cell Signal 15, 565-74 (2003).
30. Glavas, N.A., Ostenson, C., Schaefer, J.B., Vasta, V., Beavo, J.A. T cell activation upregulates cyclic nucleotide phosphodiesterases 8A1 and 7A3. PNAS 98, 6319-6324 (2001).
31. Hansen, R.S. & Beavo, J.A. Purification of two calcium/calmodulin-dependent forms of cyclic nucleotide phosphodiesterase by using conformation-specific monoclonal antibody chromatography. *Proc Natl Acad Sci U S A* **79**, 2788-2792 (1982).
32. Hansen, R.S. & Beavo, J.A. Differential recognition of calmodulin-enzyme complexes by a conformation-specific anti-calmodulin monoclonal antibody. *J Biol Chem* **261**, 14636-14645 (1986).
33. Hayes, J.S., Brunton, L.L. & Mayer, S.E. Selective activation of particulate cAMP-dependent protein kinase by isoproterenol and prostaglandin E1. *J Biol Chem* **255**, 5113-5119 (1980).
34. Houslay, M.D., Adams D.R. PDE4 cAMP phosphodiesterases: modular enzymes that orchestrate signalling cross-talk, desensitization and compartmentalization. Biochem. J. 370, 1-18 (2003).
35. Houslay, M.D., Baillie, G.S. & Maurice, D.H. cAMP-Specific phosphodiesterase-4

enzymes in the cardiovascular system: a molecular toolbox for generating compartmentalized cAMP signaling. *Circ Res* **100**, 950-966 (2007).
36. Jeon, Y.H. *et al.* Phosphodiesterase: overview of protein structures, potential therapeutic applications and recent progress in drug development. *Cell Mol Life Sci* **62**, 1198-1220 (2005).
37. Johnson, B.D., Scheuer, T. & Catterall, W.A. Voltage-dependent potentiation of L-type Ca2+ channels in skeletal muscle cells requires anchored cAMP-dependent protein kinase. *Proc Natl Acad Sci U S A* **91**, 11492-11496 (1994).
38. Johnson, K.R., Nicodemus-Johnson, J. & Danziger, R.S. An evolutionary analysis of cAMP-specific Phosphodiesterase 4 alternative splicing. *BMC Evol Biol* **10**, 247 (2010).
39. Kamenetsky, M. *et al.* Molecular details of cAMP generation in mammalian cells: a tale of two systems. *J Mol Biol* **362**, 623-639 (2006).
40. Kamenetsky, M. *et al.* Molecular details of cAMP generation in mammalian cells: a tale of two systems. *J Mol Biol* **362**, 623-639 (2006).
41. Kapiloff, M.S. *et al.* An adenylyl cyclase-mAKAPbeta signaling complex regulates cAMP levels in cardiac myocytes. *J Biol Chem* **284**, 23540-23546 (2009).
42. Ke, H. Implications of PDE4 structure on inhibitor selectivity across PDE families. *Int J Impot Res* **16 Suppl 1**, S24-27 (2004).
43. Koyanagi, M. *et al.* Ancient gene duplication and domain shuffling in the animal cyclic nucleotide phosphodiesterase family. *FEBS Lett* **436**, 323-328 (1998).
44. Le Jeune, I.R., Shepherd, M., Van Heeke, G., Houslay, M.D. & Hall, I.P. Cyclic AMP-dependent transcriptional up-regulation of phosphodiesterase 4D5 in human airway smooth muscle cells. Identification and characterization of a novel PDE4D5 promoter. *J Biol Chem* **277**, 35980-35989 (2002).
45. Lynch, M.J. *et al.* RNA silencing identifies PDE4D5 as the functionally relevant cAMP phosphodiesterase interacting with beta arrestin to control the protein kinase A/AKAP79-mediated switching of the beta2-adrenergic receptor to activation of ERK in HEK293B2 cells. *J Biol Chem* **280**, 33178-33189 (2005).
46. Ma, W. *et al.* Ca2+, cAMP, and transduction of non-self perception during plant immune responses. *Proc Natl Acad Sci U S A* **106**, 20995-21000 (2009).
47. Mackenzie, K.F. *et al.* Human PDE4A8, a novel brain-expressed PDE4 cAMP-specific phosphodiesterase that has undergone rapid evolutionary change. *Biochem J* **411**, 361-369 (2008).
48. MacKenzie, S.J., Baillie, G.S., McPhee, I., Bolger, G.B. & Houslay, M.D. ERK2 mitogen-activated protein kinase binding, phosphorylation, and regulation of the PDE4D cAMP-specific phosphodiesterases. The involvement of COOH-terminal docking sites and NH2-terminal UCR regions. *J Biol Chem* **275**, 16609-16617 (2000).
49. MacKenzie, S.J. *et al.* Long PDE4 cAMP specific phosphodiesterases are activated by protein kinase A-mediated phosphorylation of a single serine residue in Upstream Conserved Region 1 (UCR1). *Br J Pharmacol* **136**, 421-433 (2002).
51. Makranz, C., Cohen, G., Reichert, F., Kodama, T. & Rotshenker, S. cAMP cascade (PKA, Epac, adenylyl cyclase, Gi, and phosphodiesterases) regulates myelin phagocytosis mediated by complement receptor-3 and scavenger receptor-AI/II in microglia and macrophages. *Glia* **53**, 441-448 (2006).
52. Martinez-Atienza, J., Van Ingelgem, C., Roef, L. & Maathuis, F.J. Plant cyclic nucleotide signalling: facts and fiction. *Plant Signal Behav* **2**, 540-543 (2007).
53. Moglich, A., Ayers, R.A., Moffat, K. Structure and Signaling Mechanism of Per-ARNT-Sim Domains. Structure 17, 1282-1294 (2009).

54. Owen, D.M., Magenau, A., Williamson, D. & Gaus, K. The lipid raft hypothesis revisited - New insights on raft composition and function from super-resolution fluorescence microscopy. *Bioessays* **34**, 739-747 (2012).
55. Owen, D.M. *et al.* PALM imaging and cluster analysis of protein heterogeneity at the cell surface. *J Biophotonics* **3**, 446-454 (2010).
56. Patrucco, E., Albergine, M.S., Santana, L.F., Beavo, J.A. Phosphodiesterase 8A (PDE8A) regulates excitation-contraction coupling in ventricular myocytes. J. Mol. Cell. Cardiol. 49, 330-333 (2010).
57. Pawson, T. & Scott, J.D. Signaling through scaffold, anchoring, and adaptor proteins. *Science* **278**, 2075-2080 (1997).
58. Perry, S.J., Baillie, G.S., Kohout, T.A., McPhee, I., Magiera, M.M., Ang, K.L. et al. Targeting of cyclic AMP degradation to beta(2)-adrenergic receptors by beta-arrestins. Science 298, 834-836 (2002).
59. Rena, G. *et al.* Molecular cloning, genomic positioning, promoter identification, and characterization of the novel cyclic amp-specific phosphodiesterase PDE4A10. *Mol Pharmacol* **59**, 996-1011 (2001).
60. Richter, W. 3',5' Cyclic nucleotide phosphodiesterases class III: members, structure, and catalytic mechanism. *Proteins* **46**, 278-286 (2002).
61. Richter, W., Jin, S.L. & Conti, M. Splice variants of the cyclic nucleotide phosphodiesterase PDE4D are differentially expressed and regulated in rat tissue. *Biochem J* **388**, 803-811 (2005).
62. Serezani, C.H., Ballinger, M.N., Aronoff, D.M. & Peters-Golden, M. Cyclic AMP: master regulator of innate immune cell function. *Am J Respir Cell Mol Biol* **39**, 127-132 (2008).
63. Serezani, C.H. *et al.* Prostaglandin E2 suppresses bacterial killing in alveolar macrophages by inhibiting NADPH oxidase. *Am J Respir Cell Mol Biol* **37**, 562-570 (2007).
64. Shakur, Y. *et al.* Membrane localization of cyclic nucleotide phosphodiesterase 3 (PDE3). Two N-terminal domains are required for the efficient targeting to, and association of, PDE3 with endoplasmic reticulum. *J Biol Chem* **275**, 38749-38761 (2000).
66. Soderling, S.H., Bayuga, S.J., Beavo, J.A. Cloning and characterization of a cAMP-specific cyclic nucleotide phosphodiesterase. PNAS 95, 8991-8996 (1998).
67. Tsai, L.L., Beavo, J.A. The roles of cyclic nucleotide phosphodiesterases (PDEs) in steroidogenesis. Current opinion in pharmacology 11, 670-675 (2011).
68. Vang, A.G. *et al.* PDE8 regulates rapid Teff cell adhesion and proliferation independent of ICER. *PLoS One* **5**, e12011 (2010).
69. Vasta, V., Shimizu-Albergine, M., Beavo, J.A. Modulation of Leydig cell function by cyclic nucleotide phosphodiesterase 8A. PNAS 103, 19925-30 (2006).
70. Vicini, E. & Conti, M. Characterization of an intronic promoter of a cyclic adenosine 3',5'-monophosphate (cAMP)-specific phosphodiesterase gene that confers hormone and cAMP inducibility. *Mol Endocrin*ol 11, 839-850 (1997).
71. Wang, P., Wu, P., Egan, R.W., Billah, M.M. Human phosphodiesterase 8A splice variants: cloning, gene organization, and tissue distribution. Gene 280, 183-194 (2001).
72. Wang, H., Yan, Z., Yang, S., Cai, J., Robinson, H., Ke, H. Kinetic and Structural Studies of Phosphodiesterase-8A and Implication on the Inhibitor Selectivity. Biochemistry 47, 12760–12768 (2008).
73. Willoughby, D., Masada, N., Wachten, S., Pagano, M., Halls, M.L., Everett, K.L., Ciruela, A., Cooper D.M.F. AKAP79/150 Interacts with AC8 and Regulates Ca2_-

dependent cAMP Synthesis in Pancreatic and Neuronal Systems. THE JOURNAL OF BIOLOGICAL CHEMISTRY, 285, 20328–20342 (2010).
74. Wu, P., Wang, P. Per-Arnt-Sim domain-dependent association of cAMP-phosphodiesterase 8A1 with I_B proteins. PNAS 101, 17634-9 (2004).
75. Yan, Z., Wang, H., Cai, J., Ke, H. Refolding and kinetic characterization of the phosphodiesterase-8A catalytic domain. Protein Expression and Purification 64, 82–88 (2009).
76. Zhang, K.Y. *et al.* A glutamine switch mechanism for nucleotide selectivity by phosphodiesterases. *Mol Cell* **15**, 279-286 (2004).